A&A 561, A93 (2014)
DOI: 10.1051/0004-6361/201322559

Astronomy & Astrophysics

On the metallicity of open clusters

II. Spectroscopy⋆

U. Heiter[1], C. Soubiran[2], M. Netopil[3], and E. Paunzen[4]

[1] Institutionen för fysik och astronomi, Uppsala universitet, Box 516, 751 20 Uppsala, Sweden
e-mail: ulrike.heiter@physics.uu.se
[2] Université Bordeaux 1, CNRS, Laboratoire d'Astrophysique de Bordeaux UMR 5804, BP 89, 33270 Floirac, France
[3] Institut für Astrophysik der Universität Wien, Türkenschanzstrasse 17, 1180 Wien, Austria
[4] Department of Theoretical Physics and Astrophysics, Masaryk University, Kotlářská 267/2, 611 37 Brno, Czech Republic

Received 28 August 2013 / Accepted 20 October 2013

ABSTRACT

Context. Open clusters are an important tool for studying the chemical evolution of the Galactic disk. Metallicity estimates are available for about ten percent of the currently known open clusters. These metallicities are based on widely differing methods, however, which introduces unknown systematic effects.

Aims. In a series of three papers, we investigate the current status of published metallicities for open clusters that were derived from a variety of photometric and spectroscopic methods. The current article focuses on spectroscopic methods. The aim is to compile a comprehensive set of clusters with the most reliable metallicities from high-resolution spectroscopic studies. This set of metallicities will be the basis for a calibration of metallicities from different methods.

Methods. The literature was searched for [Fe/H] estimates of individual member stars of open clusters based on the analysis of high-resolution spectra. For comparison, we also compiled [Fe/H] estimates based on spectra with low and intermediate resolution. At medium and high resolution, we found that differences in the analysis methods have a stronger effect on the metallicity than that of quality differences in the observations. We retained only highly probable cluster members and introduced a restriction on atmospheric parameters.

Results. We combined 641 individual metallicity values for 458 stars in 78 open clusters from 86 publications to form our final set of high-quality cluster metallicities. The photometric metallicities discussed in the first paper of this series are systematically lower than the spectroscopic ones by about 0.1 dex, and the differences show a scatter of about 0.2 dex. In a preliminary comparison of our spectroscopic sample with models of Galactic chemical evolution, none of the models predicts the observed radial metallicity gradient.

Conclusions. Photometric metallicities show a large intrinsic dispersion, while the more accurate spectroscopic sample presented in this paper comprises fewer than half the number of clusters. Only a sophisticated combination of all available photometric and spectroscopic data will allow us to trace the metallicity distribution in the Galactic disk on a local and global scale.

Key words. Galaxy: abundances – open clusters and associations: general – stars: abundances

1. Introduction

The metallicity of stars is the key to exploring of the chemical structure and evolution of the Galaxy. But which is the best way to determine this important astrophysical parameter? High-resolution spectroscopy is often claimed to be the most accurate method (e.g. Magrini et al. 2009). It is certainly true that this is the only method available to measure abundances of individual chemical elements. However, the overall stellar metallicity can be reliably inferred by a variety of other means provided that a good calibration is available. Furthermore, the accuracy of high-resolution spectroscopy is not always assessed in a satisfactory way.

Photometry and low-resolution spectroscopic studies have the advantage of providing results for large samples within a short time (both the observations and the analysis require less time). High-resolution spectra contain significantly more information and are therefore expected to give more accurate results. However, interpreting these data is based on theoretical stellar atmospheres and modelling of spectral lines. The complete procedure of an abundance analysis requires one to specify a considerable amount of input data, assumptions for the physics of relevant processes, and a significant number of free parameters. This leads to a wide variety of possibilities to analyse a given data set, which may lead to differences in the metallicity scales published by different research groups.

We set out to investigate to which extent this is the case, thus testing the *accuracy* of spectroscopic stellar metallicities. We note that individual metallicity studies might well be able to achieve a high *precision* for a limited number of stars (e.g. Meléndez et al. 2009), allowing one to draw important conclusions on a small subsystem of Galactic stars. But to obtain a complete picture of the Galactic chemical evolution requires one to combine the results of different authors, which will each be subject to systematic uncertainties of unknown magnitude.

⋆ Tables 1 and 4 are only available at the CDS via anonymous ftp to cdsarc.u-strasbg.fr (130.79.128.5) or via
http://cdsarc.u-strasbg.fr/viz-bin/qcat?J/A+A/561/A93

For recent studies that compared spectroscopic analyses of well-known field stars using several different methods see for instance Lebzelter et al. (2012) and Jofré et al. (2013).

We focus here on metallicity determinations of stars in open clusters (OCs). These objects have been used for a long time to investigate the radial metallicity gradient of the Galactic disk. Furthermore, the studied stars cover a wide range in stellar parameters ($T_{\rm eff}$ and $\log g$). Stars in any one cluster all formed at the same time from the same material with a unique metallicity, which provides an additional test for the consistency of the determined metallicities.

Since the 1990s, we have seen a surge of spectroscopic metallicity studies of OC stars. This probably reflects the progress in automated abundance analysis, but is certainly also an effect of the availability of efficient multi-object spectrographs, such as FLAMES at ESO's VLT or Hydra at the WIYN telescope on Kitt Peak. Open clusters are regarded as ideal probes for the chemical evolution of the Galactic disk, because they are numerous (more than 2000 presently known), are located throughout the disk, and span a wide range of ages (Dias et al. 2002). An accurate knowledge of the cluster metallicity is of twofold importance. It obviously provides a measurement point for the disk chemistry at a certain location. Second, it is important for determining the cluster age and distance (using metallicity-dependent isochrones) and thus the point in time corresponding to the particular metallicity measurement. When interpreting these measurements, it is important, however, to consider possible motions of the clusters during their lifetime (e.g. Wu et al. 2009).

In spite of the astrophysical significance, metallicity estimations for OCs are still rare. In a previous paper, we compiled photometric metallicity determinations for 188 OCs (Paunzen et al. 2010, hereafter Paper I). Recent compilations of spectroscopic metallicities include those of Magrini et al. (2009, 2010; 63 clusters) and Carrera & Pancino (2011; 89 clusters). These contain 29 clusters that are not included in our photometric sample, and thus the total current fraction of known clusters with a metallicity assessment is about 10%. The two spectroscopic compilations take different approaches to arrive at a metallicity value for each cluster. Magrini et al. selected the result of one specific publication per cluster for their sample, while Carrera & Pancino (2011) averaged all available determinations for each cluster. Both approaches suffer from the inhomogeneity inherent in data originating from many different research groups.

There are several recent attempts of constructing homogeneous sets of spectroscopic OC metallicities. Friel et al. (2010) complemented their own sample of eleven clusters with results from only three other groups and presented careful evaluations of possible differences in measurements and methods among all groups. This approach resulted in a homogeneous but small sample of 26 clusters. For the BOCCE project[1] (Bragaglia & Tosi 2006; Bragaglia et al. 2009) 45 clusters have been selected, for which age, distance, reddening, and metallicity are being determined in a homogeneous way. For most of the clusters they obtained their own photometry, and for a large portion high-resolution spectra were acquired using only a few instruments. Metallicities determined in a consistent way are published for eight clusters so far.

The most ambitious current effort is the *Gaia*-ESO Public Spectroscopic Survey (Gilmore et al. 2012, PIs Randich and Gilmore), which will obtain medium- and high-resolution spectra for about 10^5 Galactic stars during five years with one instrument (FLAMES-GIRAFFE-UVES). The target list includes stars in about 100 OCs, and major efforts are put into the preparation of a homogeneous analysis of this unprecedented dataset in a unique collaboration across more than ten research groups.

In the current paper, we aim to harvest the existing literature in the best possible way. The motivation is to obtain an up-to-date overview of the status and current limitations of OC metallicities. This is of crucial importance for the implementation of the on-going surveys (in particular the *Gaia* space mission and the *Gaia*-ESO survey) – concerning both the best selection of target clusters and target stars, and the selection of clusters and stars for calibration purposes. Our approach is to compile atmospheric parameters and spectroscopic metallicities for individual stars in each cluster and compare the results of different authors for stars in common.

The article is arranged as follows: in Sect. 2 we describe the selection of the metallicity determinations. In Sect. 3 we compare the results obtained by different authors who studied the same OCs, star-by-star as well as for the mean cluster metallicity. We also assess the importance of spectrum quality for mean cluster metallicity. In Sect. 4 we present our final high-resolution sample. In Sect. 5 we compare our sample with others and discuss possible applications of our sample to the study of Galactic structure, and Sect. 6 concludes the paper.

2. Data selection

2.1. High-resolution sample

To build a list of reference OCs with the most reliable metallicities, we first gathered individual stars – highly probable members of OCs – with atmospheric parameters determined from spectra of high resolution ($R = \lambda/\Delta\lambda$) and high signal-to-noise ratio (S/N). The lower limit in spectrum quality was set to $R = 25\,000$, and $S/N = 50$. We searched the PASTEL database (Soubiran et al. 2010) and the recent literature for such stars in references posterior to 1990 and until June 2013. Only stars with $T_{\rm eff} < 7000$ K were included to avoid rapid rotators and chemical peculiarities. All determinations not in PASTEL at the time of writing will be included in the database in the next update. We eliminated confirmed non-members, spectroscopic binaries, and chemically peculiar stars and kept only stars with a high probability of membership. Membership information was mainly based on radial-velocity criteria presented in Mermilliod et al. (2008, 2009). Criteria presented in the articles from which we gathered the spectroscopic determinations and information extracted from the WEBDA[2] (Mermilliod & Paunzen 2003) and Simbad databases were also used for membership evaluation. We started with a list of 571 stars in 86 OCs, with 830 metallicity determinations from 94 papers. In Table 1 we list the basic information for the full starting sample of cluster members, which should be sufficient to extract their parameters from the PASTEL catalogue (accessible via VizieR[3]).

For comparison purposes, we also extracted mean cluster metallicities from a number of studies (post-1990) at high resolution and low S/N (<50), and also at medium resolution ($R < 25\,000$, high and low S/N), that is, below the quality criteria defined above. Some of these determinations are discussed in Sect. 3.3 at the individual star level, and several are included

[1] http://www.bo.astro.it/~angela/bocce.html

[2] http://webda.physics.muni.cz

[3] http://vizier.u-strasbg.fr/viz-bin/VizieR?-source=B%2Fpastel

Table 2. Mean cluster metallicities and references for lower-quality studies not discussed in the paper (not in Tables 9 or 10).

High-resolution, low SNR (<50) studies						
Cluster ID	Mean [Fe/H]	std. dev.	Resolution	#	Star type	Reference
Berkeley 21	−0.54	0.20	48 000	3	giant	Hill & Pasquini (1999)
Berkeley 22	−0.32	0.19	34 000	2	giant	Villanova et al. (2005)
Berkeley 25	−0.20	0.05	40 000	4	giant	Carraro et al. (2007b)
Berkeley 66	−0.48	0.24	34 000	2	giant	Villanova et al. (2005)
Berkeley 73	−0.22	0.10	40 000	2	giant	Carraro et al. (2007b)
Berkeley 75	−0.22	0.20	40 000	1	giant	Carraro et al. (2007b)
NGC 2355	−0.07	0.11	42 000	15	giant	Soubiran et al. (2000)
Ruprecht 4	−0.09	0.05	40 000	3	giant	Carraro et al. (2007b)
Ruprecht 7	−0.26	0.05	40 000	5	giant	Carraro et al. (2007b)
Medium-resolution, high SNR (>50) studies						
Cluster ID	Mean [Fe/H]	std. dev.	Resolution	#	Star type	Reference
IC 2581	−0.34		18 000	1	giant	Luck (1994)
IC 4725	0.17	0.09	18 000	3	giant	Luck (1994)
NGC 2168	−0.21	0.10	20 000	9	dwarf	Barrado y Navascués et al. (2001)
NGC 2425	−0.15	0.09	21 000	4	giant	Jacobson et al. (2011b)
NGC 3293	0.14	0.11	∼20 000	2	giant+dwarf	Trundle et al. (2007)
NGC 4755	0.39	0.25	∼20 000	1	dwarf	Trundle et al. (2007)
NGC 6067	0.01	0.12	18 000	7	giant	Luck (1994)
NGC 6087	−0.01	0.23	18 000	3	giant	Luck (1994)
NGC 6611	0.17	0.15	20 000	1	dwarf	Trundle et al. (2007)
NGC 6882/5	−0.02	0.01	18 000	2	giant	Luck (1994)
Tombaugh 2	−0.28	0.08	21 000	7	giant	Frinchaboy et al. (2008)
Tombaugh 2	−0.31	0.02	∼17 000	13	giant	Villanova et al. (2010)
Medium-resolution, low SNR (<50) studies						
Cluster ID	Mean [Fe/H]	std. dev.	Resolution	#	Star type	Reference
NGC 1883	−0.20	0.22	20 000	2	giant	Villanova et al. (2007)
NGC 6253	0.36	0.20	15 000	2	giant	Carretta et al. (2000)
NGC 6791	0.40	0.10	20 000	1	(a)	Peterson & Green (1998)
NGC 6791	0.39	0.05	20 000	10	giant	Carraro et al. (2006)

Notes. (a) blue-straggler or blue-horizontal-branch star.

in Sect. 3.7 at the cluster level. The remaining determinations are not further discussed in this paper. For future reference, we list them in Table 2.

2.2. Low-resolution sample

As low-resolution spectroscopic metallicity investigations we considered spectra taken at $R \approx 1000{-}2000$, from which spectroscopic indices, that is, the strength of absorption features, were measured (predominantly Fe I and Fe peak blends). A calibration giving the index strength as a function of the atmospheric parameters allows one to determine the metallicity. Low-resolution studies of OC stars are relatively rare in the literature. In addition to a query within ADS, the bibliography of the OC database WEBDA was used, and references in high-resolution studies were checked in this respect. We found Friel & Janes (1993), Thogersen et al. (1993), Friel et al. (2002), Worthey & Jowett (2003), and Marshall et al. (2005), the first three of which claim to be on the same metallicity scale. Since Friel et al. (2002) revised the results of the former two studies in combination with new data, we included only their metallicity determinations of 39 OCs in total. Additionally, we adopted the result for the cluster NGC 6705, investigated by Thogersen et al. (1993), which is not listed in Friel et al. (2002) due to their restriction to ages older than 0.7 Gyr. Friel et al. (2002) and Marshall et al. (2005) determined [Fe/H] based on spectroscopic indices defined in Friel (1987)[4]. Worthey & Jowett (2003) used seven indices on the Lick/IDS system defined in Worthey et al. (1994).

Worthey & Jowett (2003), and Marshall et al. (2005) seem to present a higher metallicity scale than Friel et al. (2002). Worthey & Jowett (2003) studied two clusters (NGC 188 and NGC 6791) and obtained a metallicity about 0.2 dex higher than Friel et al. (2002) for both clusters. Marshall et al. (2005) have three clusters (out of seven) in common with Friel et al. (2002), indicating a similar tendency (an offset between 0.1 and 0.2 dex). The only exception is NGC 6705, for which the result of Marshall et al. (2005) is slightly lower than that of Thogersen et al. (1993, they agree within the errors).

In total, we found 49 metallicity values for 43 individual clusters investigated with low-resolution spectroscopy, of which 34 are also included in the high-resolution sample. Four of the low-resolution clusters have neither photometric nor high-resolution spectroscopic metallicities. Some of these determinations are discussed in Sects. 3.2 to 3.4 and in Sect. 3.7. The remaining determinations are not discussed in this paper. For future reference, we list them in Table 3. A detailed comparison of these results, and if possible, a recalibration by means of the high-resolution sample, is planned for the next paper in this series.

[4] Six and eleven indices were used in the two works, respectively.

Table 3. Mean cluster metallicities for low-resolution studies of giant stars in clusters not discussed in the paper (not in Table 9).

Cluster ID	Mean [Fe/H]	std. dev.	#	First author	Cluster ID	Mean [Fe/H]	std. dev.	#	First author
Berkeley 17	–0.33	0.12	13	Friel	NGC 2099	0.05	0.14	8	Marshall
Berkeley 20	–0.61	0.14	6	Friel	NGC 2141	–0.33	0.10	6	Friel
Berkeley 21	–0.62	0.11	4	Friel	NGC 2324	–0.06	0.07	4	Marshall
Berkeley 31	–0.40	0.16	17	Friel	NGC 2324	–0.15	0.16	7	Friel
Berkeley 32	–0.50	0.04	10	Friel	NGC 2360	–0.26	0.02	4	Friel
Collinder 261	–0.16	0.13	21	Friel	NGC 2477	–0.13	0.10	28	Friel
IC 166	–0.34	0.16	4	Friel	NGC 2506	–0.44	0.06	5	Friel
King 5	–0.30	0.17	19	Friel	NGC 2539	–0.04	0.05	4	Marshall
King 8	–0.39		1	Friel	NGC 3680	–0.19	0.05	7	Friel
King 11	–0.27	0.15	16	Friel	NGC 3960	–0.34	0.09	5	Friel
Melotte 66	–0.47	0.09	4	Friel	NGC 6819	–0.11	0.06	7	Friel
NGC 188	–0.10	0.09	21	Friel	NGC 6819	0.07	0.24	4	Marshall
NGC 188	0.08	0.05	14	Worthey	NGC 6940	–0.12	0.10	6	Friel
NGC 752	–0.18	0.04	9	Friel	Pismis 2	–0.07	0.23	9	Friel
NGC 1193	–0.51	0.09	4	Friel	Tombaugh 2	–0.44	0.09	12	Friel

References. Friel et al. (2002); Worthey & Jowett (2003); Marshall et al. (2005).

3. Assessment of spectroscopic metallicities

3.1. Mean metallicities and quoted errors for the high-resolution sample

A significant number of individual OCs in the high-resolution sample were studied by different authors with different instruments, methods, and line lists. Throughout this article, we use the term *metallicity* synonymously with *iron abundance*, [Fe/H]. Different authors used different approaches for determining the iron abundances – using either only Fe I lines or only Fe II lines, or both. If abundances for both ions are given, we used the metallicity value as given by the authors, which can be either an unweighted mean of Fe I and Fe II abundances or a mean weighted by the number of lines used in each case. In the few cases where metallicity values for individual stars are not clearly stated, we formed an unweighted mean of Fe I and Fe II abundances. In the majority of the publications the metallicity is based on Fe I only. In about 10% of the cases a weighted mean is given. Another 10% achieved ionization equilibrium in the analysis by adapting the atmospheric parameters to such an extent that the Fe I and Fe II abundances agree exactly. There is also a strong variation in the number of Fe lines used for the analysis, which can be anything between two and 130 Fe I lines (and individual publications with 180 or 265 lines), and one to 15 Fe II lines (40 lines in one publication).

These variations are partly due to the different telescopes and instruments used to obtain the observed spectra, in particular their wavelength coverage. The observations were obtained at about 30 different telescopes, most of them in the 2–4 m class, and a few at 8–10 m. Echelle spectrographs were used for most observations, providing a large wavelength coverage, but settings focusing on different parts of the optical region were used. The minimum wavelength of the spectra varies between publications from 360 to 700 nm, and the maximum wavelength from 600 to 1060 nm.

We show the individual metallicities averaged by OC and by reference in Fig. 1 and list them in Table 4. The figure shows a certain lack of homogeneity for the clusters studied by several authors. The errors on individual [Fe/H] determination quoted by the authors are typically around 0.1 dex, and for most determinations they are less 0.2 dex (see Fig. 2). Only 14 determinations for seven clusters in six papers have quoted metallicity errors between 0.25 and 0.35 dex (Berkeley 22: Jacobson & Friel 2013; Berkeley 29 and NGC 2141: Yong et al. 2005; see also Sect. 3.6; Collinder 261: Friel et al. 2003; see also Sect. 3.5; NGC 2112: Brown et al. 1996; see also Sect. 3.7; NGC 3680: Pasquini et al. 2001; see also Sect. 3.4; NGC 6705: Santos et al. 2012). For 81 determinations, the authors do not quote any error for the metallicity. There is a weak dependence of errors on $T_{\rm eff}$ and [Fe/H], such that the largest errors are quoted for stars with $T_{\rm eff} < 5000$ K and [Fe/H] < -0.1 dex.

We note that the errors quoted by most authors are in fact the standard deviations of the abundances determined from the selected Fe lines, with the exception of Pancino et al. (2010) and Carrera & Pancino (2011). These authors quote the standard error of the line abundances, and we multiplied their errors by the square root of the number of lines used. The uncertainty in stellar parameters causes an additional uncertainty in the Fe abundances. This type of external error is typically estimated to be 0.1 dex in the publications included in this work. An additional source of systematic differences between different studies might arise from the choice of the solar reference metallicity. We did not assess the extension of this effect for each individual paper. However, for the studies that are based on a differential analysis with respect to a solar spectrum or that use astrophysical oscillator strengths, the derived or adopted value of the solar Fe abundance is not important. We expect this to be the case for the majority of the publications. The remaining studies may be affected by external errors of up to 0.1 dex.

Standard deviations of the mean cluster metallicity from each individual paper are mostly lower than 0.1 dex, with a peak below 0.05 dex, which shows that the internal uncertainties of metallicity determinations are probably lower than the quoted errors (see Fig. 2). When we combine all determinations per cluster from all papers, the peak of the standard deviations is slightly higher than 0.05 dex, which suggests that external errors are inherent in the datasets. In the following sections, we investigate some cases with a large number of metallicity determinations by different authors, including low-resolution studies, and some cases with large standard deviations around the mean metallicity.

In the high-resolution sample, there are 26 OCs for which metallicity determinations are available for fewer than three stars. The reliability of the metallicities for these clusters is

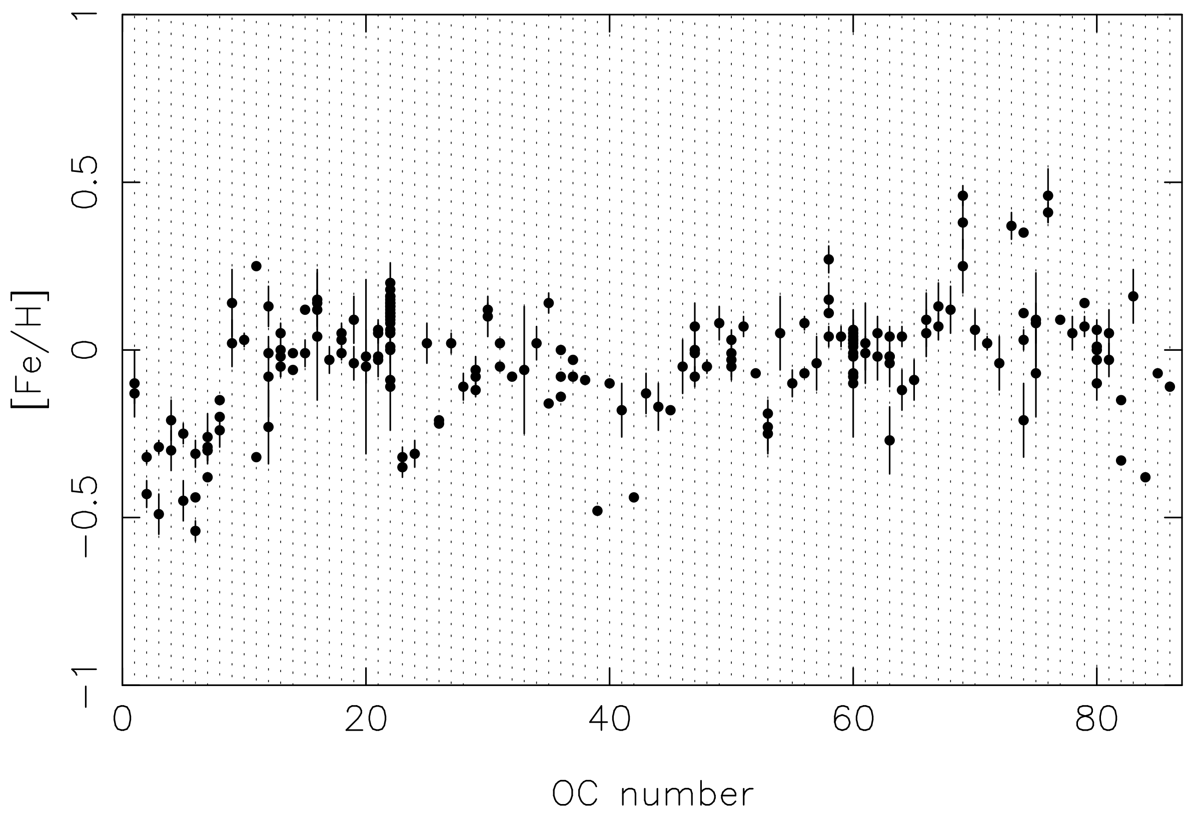

Fig. 1. Mean metallicity of OCs per publication, as listed in Table 4.

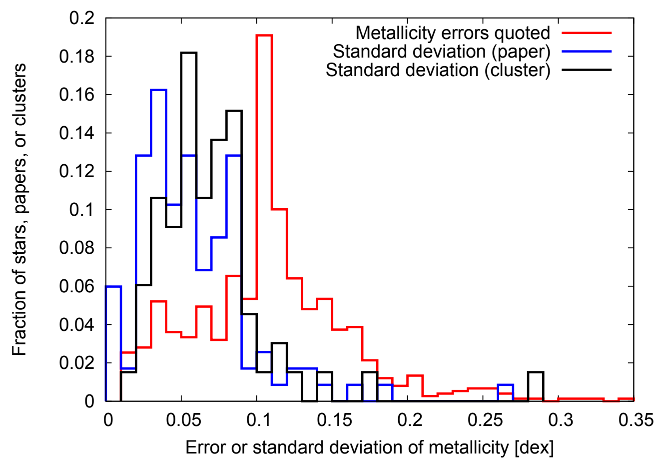

Fig. 2. Distribution of metallicity errors quoted by authors (red line) compared with the distributions of standard deviations for mean metallicities per cluster for each paper (blue line), and for all papers (black line), combining determinations for at least three stars.

difficult to assess. We will apply the conclusions drawn from the comparisons for the well-studied clusters[5] to these poor-studied ones for the selection of the final spectroscopic OC metallicity sample.

3.2. Solar-metallicity cluster: M67

Metallicities for *giant* stars ($\log g \leq 3.0$) in M67 (NGC 2682) have been determined in a considerable number of publications since 1990, including the low-resolution studies by Friel et al. (2002) and Marshall et al. (2005). Seven studies published after 1990 are based on high-resolution, high-S/N spectra. We plot the metallicities determined for ten individual giant stars by more than one author at high and low resolution in Fig. 3 as a function of reference $T_{\rm eff}$ (see figure caption for references). The reference $T_{\rm eff}$ values were taken from Tautvaišiene et al. (2000) except for Fagerholm 286 (average of Santos et al. 2009 and Pancino et al. 2010). Each $T_{\rm eff}$ value corresponds to one star, except for $T_{\rm eff}$ = 4730 K, which corresponds to two stars. The reference $T_{\rm eff}$ values agree to within 100 K with those given in the individual publications. The internal uncertainties for the individual [Fe/H] values quoted by the authors range from 0.04 (Reddy et al. 2013) to 0.17 dex (Jacobson & Friel 2013), with a mean of 0.12 dex. In addition, we show metallicity determinations for four of these stars from two studies made before CCD detectors became available (Cohen 1980; Foy & Proust 1981), which are based on somewhat lower-resolution spectra, and atmospheric models and atomic data available at that time.

It is obvious that the metallicity determined from spectroscopic indices (Friel et al. 2002) is on a more metal-poor scale than the high-resolution metallicities (~0.1 dex difference). One of the older studies (Cohen 1980, $R \approx 17\,000$) shows a large systematic offset from the high-resolution studies, while the other one (Foy & Proust 1981) agrees very well. All but five of the high-resolution metallicities are confined within ±0.06 dex, with no obvious dependence on resolution or $T_{\rm eff}$. Friel et al. (2010, Sect. 6.1.1) compared their results for three stars (Fagerholm 105, 141, and 170) with three other studies (for Fe as well as other elements), and arrived at similar conclusions. The extended comparison presented here indicates that older abundance-analysis techniques applied to solar metallicity giant stars have larger systematic uncertainties than modern ones (post-1990).

[5] The starting sample contains 47 clusters with 3 to 10 stars, 10 clusters with 12 to 20 stars, 2 clusters with 29 stars, and one with 76.

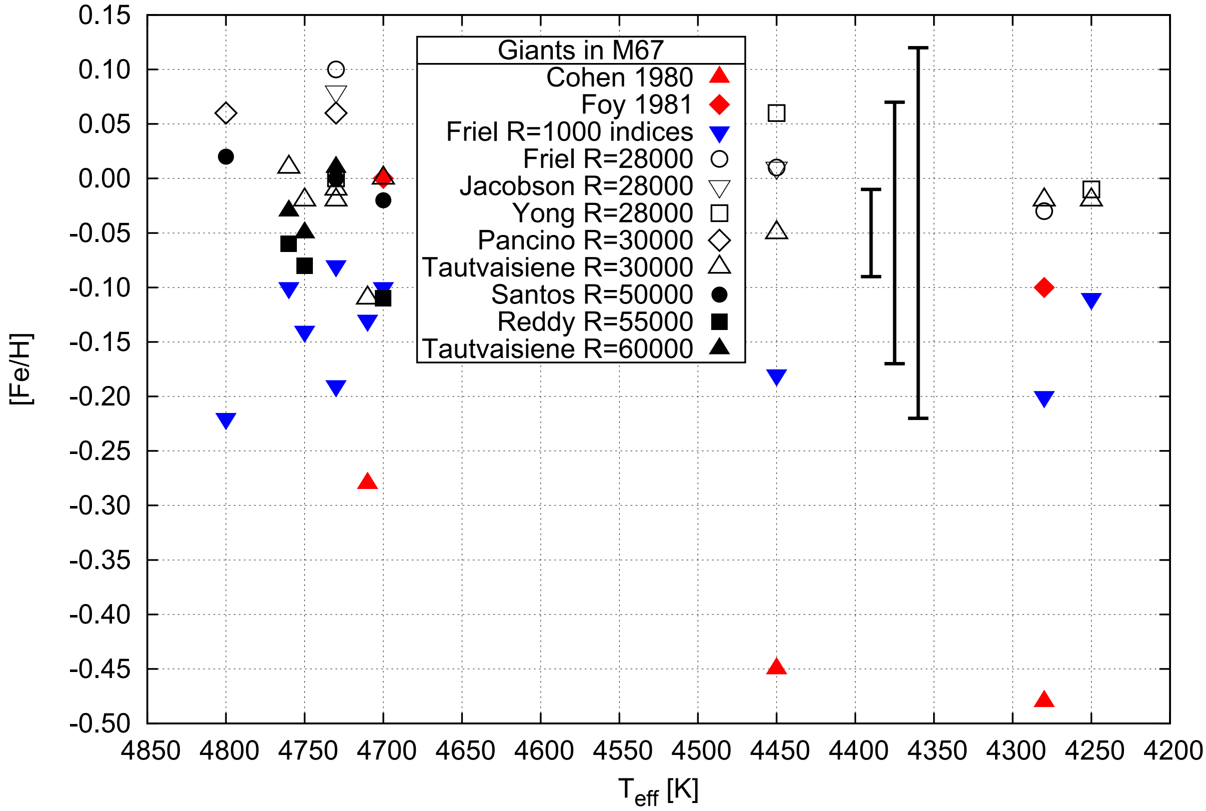

Fig. 3. Metallicity versus reference $T_{\rm eff}$ for individual giant stars in NGC 2682 (M67) that were analysed by more than one author using high- and low-resolution spectra. The metallicities are taken from the following publications: Cohen (1980); Foy & Proust (1981); Tautvaišiene et al. (2000); Friel et al. (2002); Yong et al. (2005); Santos et al. (2009); Pancino et al. (2010); Friel et al. (2010); Jacobson & Friel (2013); and Reddy et al. (2013). Data for the following stars are shown (reference $T_{\rm eff}$, number from Fagerholm 1906): (4250, 108); (4280, 170); (4450, 105); (4700, 164); (4710, 224); (4730, 141); (4730, 266); (4750, 84); (4760, 151); and (4800, 286). The bars on the upper right indicate minimum, mean, and maximum uncertainties for the individual [Fe/H] values quoted in the publications.

For *dwarf* stars in M67 we found metallicities in six publications, all based on high-resolution and high S/N spectra. Ten dwarf stars were analysed by at least two authors. We plot the metallicities determined for these stars in Fig. 4 as a function of reference $T_{\rm eff}$ on the same vertical scale as in Fig. 3 for the giant stars (see figure caption for references). The reference $T_{\rm eff}$ values are averages of the determinations from different works. Each $T_{\rm eff}$ value corresponds to one star, except for $T_{\rm eff} = 6100$ K, which corresponds to two stars (see figure caption). The reference $T_{\rm eff}$ values agree to within 100 K with those given in the individual publications. The quoted uncertainties for the individual [Fe/H] values range from 0.03 (Randich et al. 2006) to 0.13 dex (Hobbs & Thorburn 1991).

Among the dwarf analyses, the oldest study by Hobbs & Thorburn (1991) stands out among the others because it shows the largest dispersion. Otherwise, the spread in abundances is the same as for the giant stars. The lower-resolution metallicities agree with the others, but the small number of these points does not allow a general conclusion. The star with the highest temperature (Sanders 997) is an M67 blue straggler and a probable spectroscopic binary star (Shetrone & Sandquist 2000). A comparison of dwarf and giant metallicities for this extraction from the starting sample of cluster members results in equal mean values within the standard deviations (cf. Sect. 4 for a comparison based on the full final sample). The mean of the 28 post-1990 high-resolution values for giants (full and open black symbols in Fig. 3) is -0.01 ± 0.05 dex, while the mean of the 15 most recent high-resolution values for dwarfs (full black symbols in Fig. 4) is 0.02 ± 0.04 dex.

3.3. Metal-rich cluster: NGC 6791

For NGC 6791, we found five publications since 1990 with metallicity determinations for 18 giant stars appearing in at least two of them. We plot the metallicities determined for these stars in Fig. 5 as a function of reference $T_{\rm eff}$ on the same vertical and horizontal scale as in Fig. 3 for the M67 giant stars (see figure caption for references). The reference $T_{\rm eff}$ values are averages of the determinations from different works. Each $T_{\rm eff}$ value corresponds to one star (see figure caption). The reference $T_{\rm eff}$ values agree to within 100 K with those given in the individual publications. The minimum and maximum uncertainties for the individual [Fe/H] values were found in two low-resolution studies and represent the standard deviations of metallicities determined from several indices (0.01 dex in Worthey & Jowett 2003; and 0.2 dex in Friel et al. 2002). There are no multiple metallicity determinations available for dwarf stars in this cluster.

Again, the values from spectroscopic indices by Friel et al. (2002) are lower than the others, by a larger amount than at solar metallicity (~0.3 dex). However, the indices-based metallicities by Worthey & Jowett (2003) are close to the values derived from higher-resolution spectra. There is one star in common between the medium- and high-resolution studies of Geisler et al. (2012), Carraro et al. (2006), and Gratton et al. (2006), where the highest-resolution study gives the highest metallicity. The error quoted by Gratton et al. (2006) is twice as large as the difference, however, and thus the difference is not significant. Nine additional stars are in common between Geisler et al. (2012) and Carraro et al. (2006), and for all except two stars, the

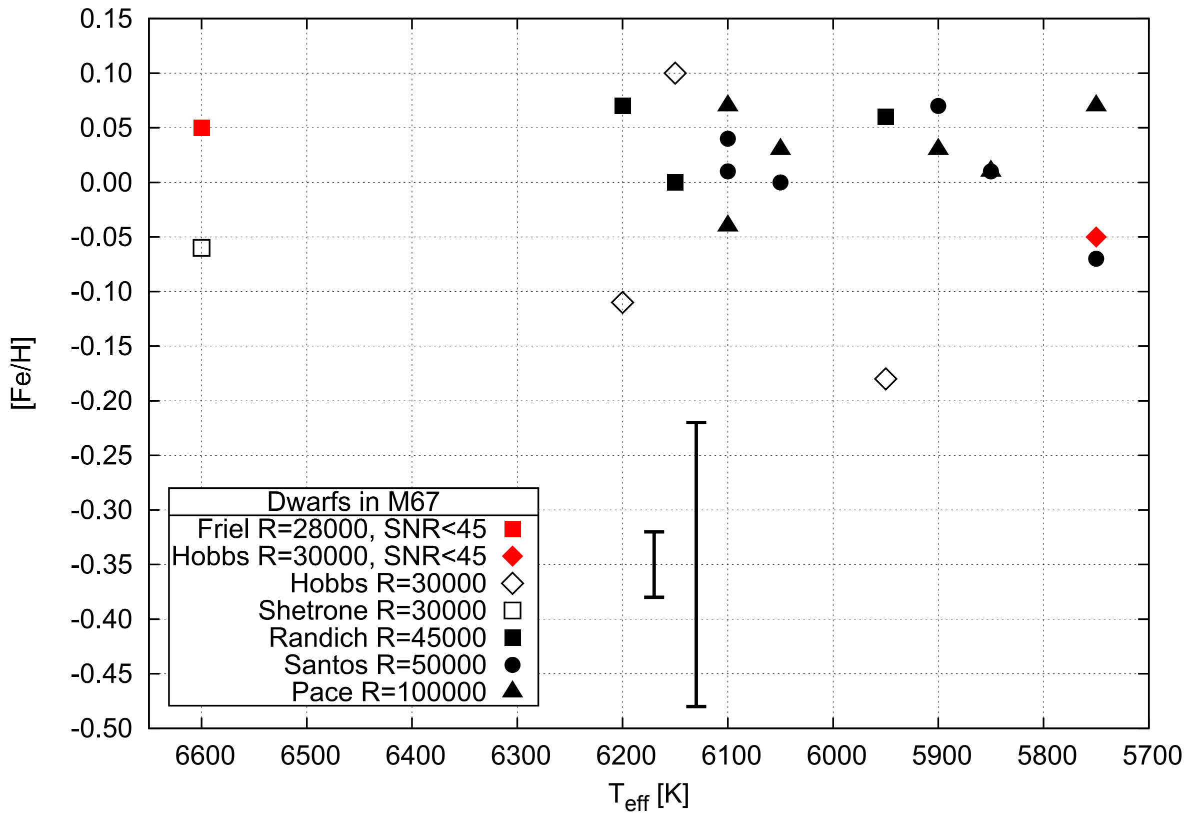

Fig. 4. Same as Fig. 3, for *dwarf* stars in M67 (NGC 2682). The metallicities are taken from the following publications: Hobbs & Thorburn (1991); Friel & Boesgaard (1992); Shetrone & Sandquist (2000); Randich et al. (2006); Pace et al. (2008); and Santos et al. (2009). Data for the following stars are shown (reference $T_{\rm eff}$, number from Sanders 1977): (5750, 746); (5850, 1255); (5900, 1048); (5950, 1256); (6050, 1283); (6100, 1092); (6100, 1287); (6150, 994); (6200, 998); and (6600, 997). The S/N of the spectra used in the different publications is higher than 50, except when stated otherwise. The bars to the right of the legend indicate minimum and maximum uncertainties for the individual [Fe/H] values quoted in the publications.

metallicities agree very well. The mean metallicity values derived from the whole samples of these publications show differences similar to the standard deviations. Geisler et al. (2012) determined [Fe/H] = 0.42 ± 0.05 for 16 stars, Carraro et al. (2006) determined [Fe/H] = 0.38 ± 0.02 for ten stars, and Gratton et al. (2006) determined [Fe/H] = 0.47 ± 0.07 for four stars[6]. These differences are probably not caused by the different resolutions, because the analysis of five subgiants at R = 45 000 by Geisler et al. (2012) results in a mean metallicity that agrees with all three of the medium- and high-resolution studies of giants within the standard deviations (see Table 4). Reasons for the differences could be the different instruments used (Hydra at WIYN and SARG at TNG), different stellar samples, different spectrum synthesis codes, and different line lists (Gratton et al. 2006 used the broadest wavelength range).

3.4. Metal-poor clusters

To evaluate the influence of spectrum quality and analysis methods on the metallicities of metal-poor clusters, we compared results from 13 publications since 1990 for giant stars appearing in ten different clusters. For these clusters, at least one determination gives a value of [Fe/H] = −0.3 dex or lower. We plot the metallicities determined for the individual stars in Fig. 6 as a function of $T_{\rm eff}$ (see figure caption for references). The reference $T_{\rm eff}$ values are taken from the works with highest resolution (or are averages from works with the same resolution). Each $T_{\rm eff}$ value corresponds to one star, except for $T_{\rm eff}$ = 4100 K in the lower panel and 4660 K in the upper panel, which correspond to two stars each. The reference $T_{\rm eff}$ values and identifications of the stars are listed in Table 5. The reference $T_{\rm eff}$ values agree to within 200 K with those given in the individual publications. The quoted uncertainties for the individual [Fe/H] values range from 0.08 (Santos et al. 2009) to 0.3 dex (Pasquini et al. 2001; Jacobson & Friel 2013), and the mean of the uncertainties for high-resolution studies is 0.17 dex.

For these clusters, we can mainly compare the metallicities by Friel & Janes (1993; Melotte 66, Berkely 21) and Friel et al. (2002) based on spectroscopic indices to the high-resolution metallicities. The mean star-by-star difference for 14 stars (excluding two stars in Pasquini et al. 2001) is −0.16 ± 0.07 dex, intermediate between the differences for M67 and NGC 6791 (both at higher metallicity).

Five of the stars appear in two or more high-resolution studies that are based on different observations: Berkeley 29 BHT 398, Berkeley 20 MPJF 8, and Berkeley 32 KM 17, as well as two stars in NGC 3680 (discussed below). For the two stars in Berkeley 29 and Berkeley 20, the study by Sestito et al. (2008; S/N = 25–50 and 40–80, respectively) resulted in higher metallicities (by 0.14 dex) than the studies by Carraro et al. (2004) and Yong et al. (2005; S/N = 70 and 56, respectively), while the determinations for the star in Berkeley 32 by Sestito et al. (2006) and Carrera & Pancino (2011) are in excellent agreement. There

[6] Note that Stetson 8082 is not included in Table 4 because its S/N is lower than 50.

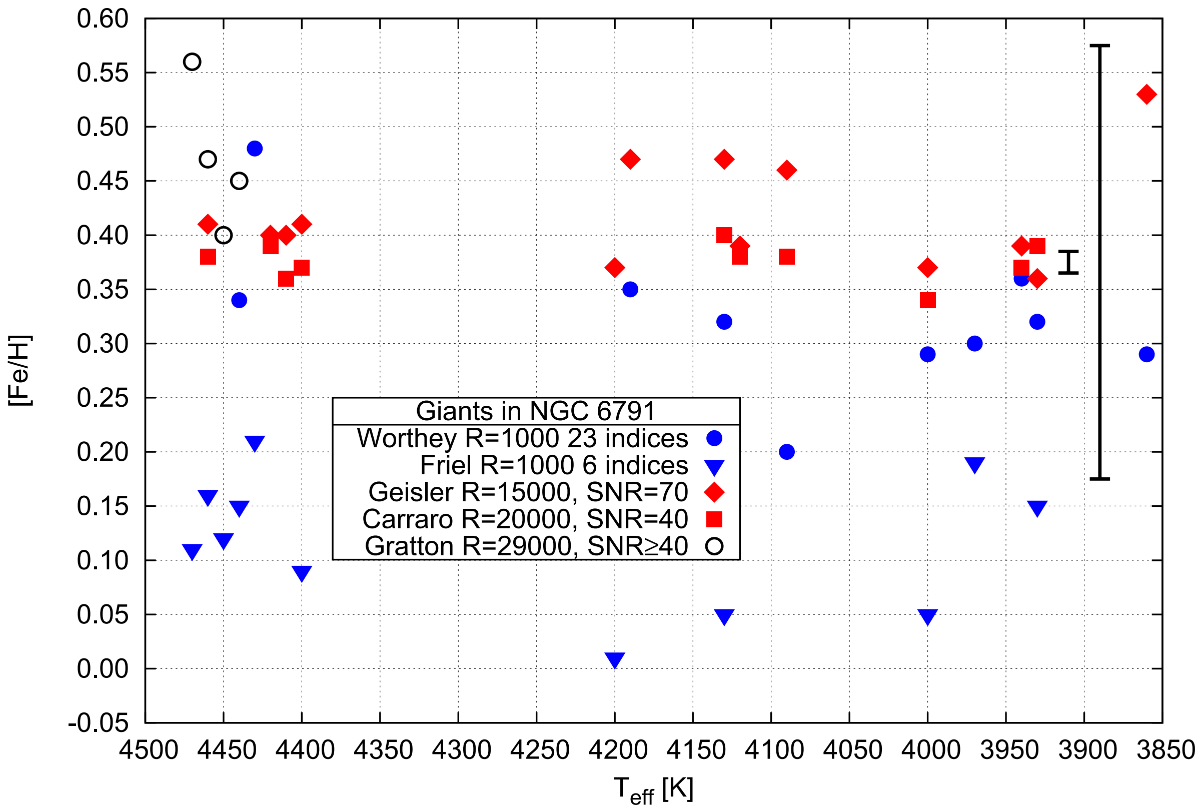

Fig. 5. Same as Fig. 3, for giant stars in NGC 6791. The metallicities are taken from the following publications: Worthey & Jowett (2003); Friel et al. (2002); Geisler et al. (2012); Carraro et al. (2006); and Gratton et al. (2006). Data for the following stars are shown (reference $T_{\rm eff}$ in K, star number from Stetson et al. 2003): (3860, 8904); (3930, 7972); (3940, 8266); (3970, 5342); (4000, 11 814); (4090, 8563); (4120, 10 898); (4130, 8988); (4190, 4952); (4200, 6288); (4400, 3369); (4410, 4715); (4420, 7922); (4430, 2723); (4440, 9462); (4450, 10 806); (4460, 8082); and (4470, 9316). The bars on the right indicate minimum and maximum uncertainties for the individual [Fe/H] values quoted in the publications.

are two other stars in Berkeley 32 (at $T_{\rm eff}$ = 4100 K), for which Friel et al. (2010) and Jacobson & Friel (2013) analysed the same observed spectra at R = 30 000 and obtained consistent metallicities. On the other hand, the lower panel of Fig. 6 shows nine stars in five clusters, for which Yong et al. (2012) and Jacobson & Friel (2013) analysed the same spectra at R = 47 000. The derived metallicities are systematically different by 0.14 dex. Note that the largest differences of about 0.2 dex are seen for the two stars with $T_{\rm eff}$ < 4000 K.

At this point, we refer to the extensive comparison work presented by Friel et al. (2010, Appendix) for Berkeley 32. They used the line lists and equivalent widths measured for nine stars by Sestito et al. (2006) and determined abundances and atmospheric parameters with their own methods. A detailed discussion of the possible effects of variations in individual analysis ingredients is given. For one star (KM 18), they independently measured equivalent widths in the spectrum used by Sestito et al. (2006) and found excellent agreement. On the other hand, using different selections of lines for the abundance determination (for a fixed set of atmospheric parameters) resulted in [Fe/H] differences of up to 0.15 dex.

For NGC 3680, the metallicities from high-resolution studies cluster around two significantly different values (No. 63 in Table 4): Santos et al. (2009) obtained a solar value (based on three giant and two dwarf stars), close to the results by Smiljanic et al. (2009) for one of the three giants and the results of Pace et al. (2008) for the same two dwarfs at R = 100 000. On the other hand, Pasquini et al. (2001) determined low metallicities ([Fe/H] ≈ −0.3 dex) for six giant stars, which include the three stars studied by Santos et al. (2009) and Smiljanic et al. (2009, see Fig. 6). First, we note that Pasquini et al. (2001) quoted metallicity errors of 0.25 to 0.35 dex, which are among the largest quoted in any publication. These errors were computed in an unconventional way – standard deviations of line abundances (interpreted as random errors due to uncertainties in equivalent widths and atomic parameters) were added linearly and not in quadrature to metallicity errors due to uncertainties in atmospheric parameters (estimated to be 0.18 dex). The errors are thus probably overestimated compared with those of other authors. Second, for their final cluster metallicity, Pasquini et al. (2001) excluded the star EGG 41 with the lowest metallicity, because they did not trust the $T_{\rm eff}$ value, and the star EGG 34 ([Fe/H] = −0.07 dex, not shown in Fig. 6), because they suspected it to be a binary star. This does not change the low cluster metallicity ([Fe/H] = −0.27 ± 0.03 dex). In addition, they added a +0.1 dex systematic error estimated from two Hyades stars, and quoted a final cluster metallicity of −0.17 ± 0.12 dex – closer to the other studies, but still significantly lower. Because of these discrepancies, which indicate systematic errors in the determinations by Pasquini et al. (2001), we decided to disregard these determinations for the computation of the average metallicity of NGC 3680 (Sect. 4).

3.5. *Peculiar case: Collinder 261*

The cluster Collinder 261 has been studied in four different publications, all at high resolution and high S/N. The analyses resulted in four different cluster metallicities, from −0.2

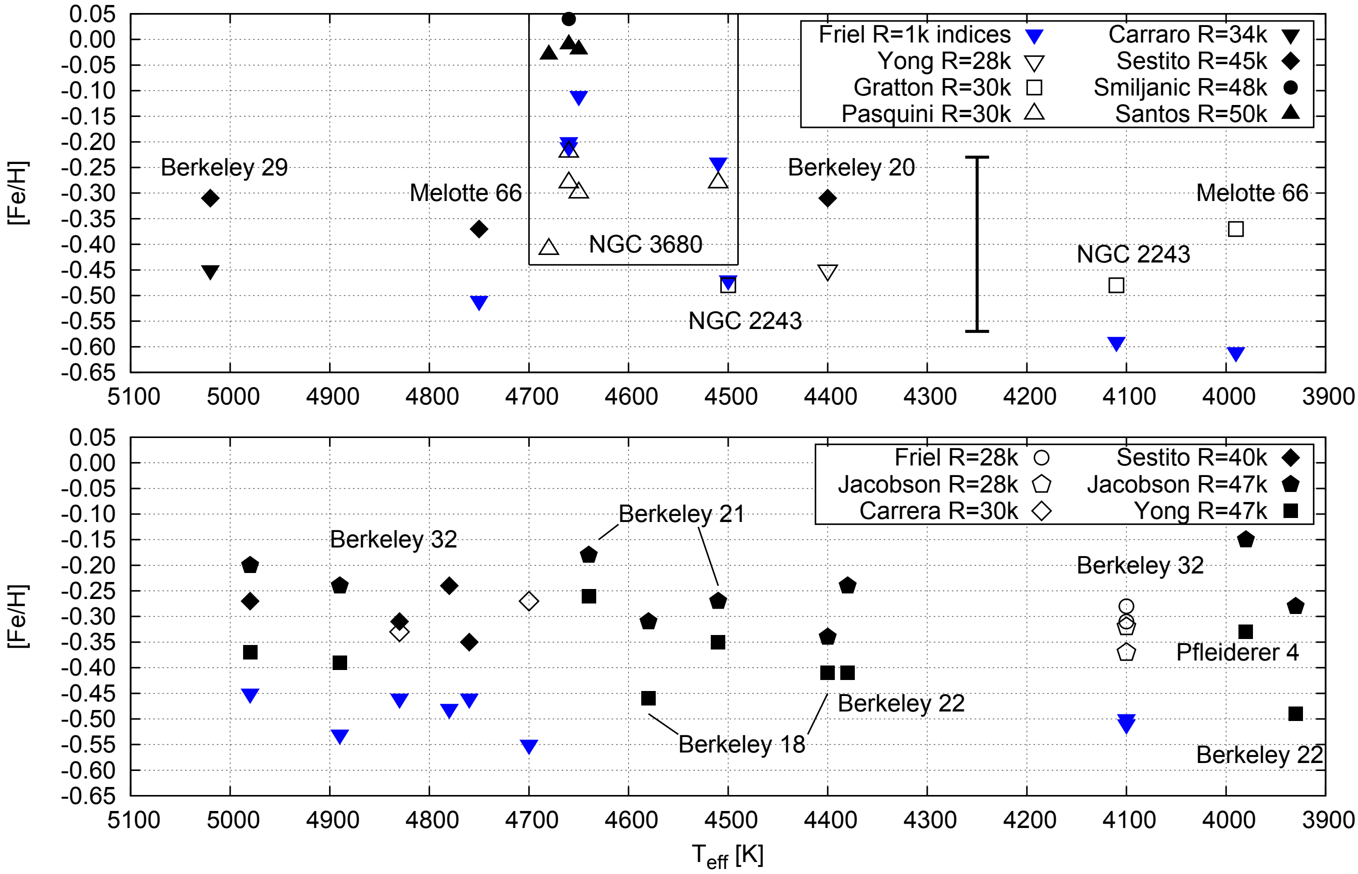

Fig. 6. Same as Fig. 3, for giant stars in ten different metal-poor clusters (five each in the *upper* and *lower panels*). The metallicities are taken from the following publications: Friel & Janes (1993); Gratton & Contarini (1994); Pasquini et al. (2001); Friel et al. (2002); Carraro et al. (2004); Yong et al. (2005); Sestito et al. (2006, 2008); Santos et al. (2009, Table 3); Friel et al. (2010); Carrera & Pancino (2011); Yong et al. (2012); and Jacobson & Friel (2013). For star identifications and corresponding reference $T_{\rm eff}$ see Table 5. The bar below the legend in the *upper panel* indicates the mean of the uncertainties for the individual [Fe/H] values quoted in the high-resolution publications (ranging from 0.04 to 0.3 dex).

to +0.1 dex in steps of 0.1 dex (No. 12 in Table 4). Figure 7 shows the metallicity determinations for individual giant stars from all four works and their [Fe/H] uncertainties. Six stars were studied by more than one author, and the data for these are connected with lines in the figure. Star identifications, data, and references are given in Table 6. All four works are based on similar-quality data from three different instruments ($S/N \approx 100$, $R \approx 45\,000$, except for Friel et al. 2003 with $R \approx 25\,000$). All four works are based on an equivalent-width analysis, and three of them used the same code for computing the model equivalent widths (MOOG, Sneden 1973). They derived the stellar atmospheric parameters in the same way, forcing excitation and ionization equilibrium on the line abundances. Thus, the diverging results obtained by these authors could be due to differences in the model atmospheres, spectral-line selection, and atomic data. Additional probable sources for discrepancies are continuum tracing and equivalent-width measurement (Sestito et al. 2008).

In three of the publications, the model atmospheres were those of R. Kurucz, although different versions were used: Carretta et al. (2005) and Sestito et al. (2008) used models from the grid on CDROM (Kurucz 1993), while De Silva et al. (2007) interpolated in the grid published by (Castelli et al. 1997). Friel et al. (2003) interpolated in the grid of Bell et al. (1976). In Table 7, we list the number of iron lines used per star and the corresponding wavelength ranges. These properties of the line lists are very similar, except for that of De Silva et al. (2007),

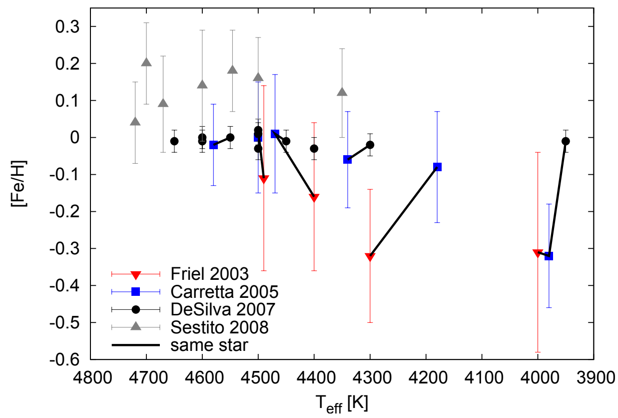

Fig. 7. Metallicity versus $T_{\rm eff}$ for individual giant stars in Collinder 261. For star identifications, data, and references see Table 6.

which includes bluer wavelengths. All four works derived metallicities with respect to a reference object. Friel et al. (2003) used oscillator-strength values derived from an Arcturus spectrum. Carretta et al. (2005) and Sestito et al. (2008) quoted their Fe abundances relative to abundances derived from a solar analysis using equivalent widths measured from high-resolution solar atlases. The homogeneity of the abundances by De Silva et al. (2007) within the cluster was achieved by a differential line-by-line abundance analysis relative to one of the cluster stars,

Table 5. Reference $T_{\rm eff}$ values and identifications of giant stars in ten different metal-poor clusters (see Fig. 6).

$T_{\rm eff}$	Cluster	ID 1		ID 2	
3930	Berkeley 22	K	643		
3980	Pfleiderer 4	RGB	1	J23505744+6220031[†]	
3990	Melotte 66	KJF	2236		4151
4100	Berkeley 32	KM	2	DBT	2689
4100	Berkeley 32	KM	4	DBT	1556
4110	NGC 2243		4209	MMU	3633
4380	Berkeley 22	K	414		
4400	Berkeley 18	K	1383		
4400	Berkeley 20	MPJF	8	SBR	1240
4500	NGC 2243		4110	MMU	1313
4510	Berkeley 21	TPM	51		415a[‡]
4510	NGC 3680	EGG	44	AHTC	1031
4580	Berkeley 18	K	1163		
4640	Berkeley 21	TPM	50		50[‡]
4650	NGC 3680	EGG	26	AHTC	3017
4660	NGC 3680	EGG	13	AHTC	3003
4660	NGC 3680	EGG	53	KGP	1873
4680	NGC 3680	EGG	41	AHTC	1050
4700	Berkeley 32	KM	12	DBT	1393
4750	Melotte 66	KJF	1953	SBR	1346
4760	Berkeley 32	KM	19	DBT	787
4780	Berkeley 32	KM	27	DBT	605
4830	Berkeley 32	KM	17	DBT	533
4890	Berkeley 32	KM	16	DBT	737
4980	Berkeley 32	KM	18	DBT	997
5020	Berkeley 29	BHT	398	FMP	948

Notes. Columns ID 1 and ID 2 give two alternative identifications, with acronyms used by the Simbad database, with some exceptions. ID 1 corresponds to the numbering system adopted by WEBDA, except for Berkeley 32 and Pfleiderer 4. [(†)] 2MASS. [(‡)] Numbering by Christian & Janes (1979).

Table 6. Atmospheric parameters and identifications of giant stars in Collinder 261 (see Fig. 7).

$T_{\rm eff}$	log g	[Fe/H]	Reference	ID	
3950	0.5	−0.01	De Silva et al. (2007)	PJM	1871
3980	0.4	−0.32	Carretta et al. (2005)	PJM	1871
4000	0.7	−0.31	Friel et al. (2003)	PJM	1871
4180	1.6	−0.08	Carretta et al. (2005)	PJM	2105
4300	1.8	−0.02	De Silva et al. (2007)	PJM	1485
4300	1.5	−0.32	Friel et al. (2003)	PJM	2105
4340	1.8	−0.06	Carretta et al. (2005)	PJM	1485
4350	1.7	+0.12	Sestito et al. (2008)	SBR	2
4400	2.1	−0.03	De Silva et al. (2007)	PJM	1481
4400	1.5	−0.16	Friel et al. (2003)	PJM	1045
4450	1.8	−0.01	De Silva et al. (2007)	PJM	1045
4470	2.1	+0.01	Carretta et al. (2005)	PJM	1045
4490	2.2	−0.11	Friel et al. (2003)	PJM	1080
4500	2.1	+0.00	Carretta et al. (2005)	PJM	1080
4500	2.1	+0.02	De Silva et al. (2007)	PJM	1080
4500	2.0	+0.01	De Silva et al. (2007)	PJM	27
4500	2.3	+0.16	Sestito et al. (2008)	SBR	6
4500	1.9	−0.03	De Silva et al. (2007)	PJM	29
4546	2.2	+0.18	Sestito et al. (2008)	SBR	7
4550	2.0	+0.00	De Silva et al. (2007)	PJM	2001
4580	1.8	−0.02	Carretta et al. (2005)	PJM	2001
4600	2.0	+0.00	De Silva et al. (2007)	PJM	1526
4600	2.0	+0.14	Sestito et al. (2008)	SBR	5
4600	2.0	−0.01	De Silva et al. (2007)	PJM	1801
4650	2.3	−0.01	De Silva et al. (2007)	PJM	1472
4670	2.2	+0.09	Sestito et al. (2008)	SBR	11
4700	2.4	+0.20	Sestito et al. (2008)	SBR	10
4720	2.1	+0.04	Sestito et al. (2008)	SBR	9

Notes. Column ID gives the star identification, with acronyms used by the Simbad database.

Table 7. Abundance analyses of Collinder 261 stars – approximate number of Fe I and Fe II lines used per star, and corresponding wavelength ranges.

	Fe I		Fe II	
Reference	n	λ [nm]	n	λ [nm]
Friel et al. (2003)	40	538–785	8	541–652
Carretta et al. (2005)	100	550–700	10	550–700
De Silva et al. (2007)	60	422–620	12	449–615
Sestito et al. (2008)	100	550–681	13	553–652

whereas the abundance zero-point was given by the adopted solar abundance from Sneden et al. (1992). These analysis approaches should minimize the uncertainties caused by atomic line data, although to different degrees. The determination of gravity could be a major source for the differences, because it relies on ionization balance between abundances from Fe I and Fe II lines. Since Fe II lines are scarce in spectra of cool stars, the derived gravity critically depends on the set of Fe II lines used and the accuracy of their equivalent widths. However, for only two of the six stars in common, there are significant differences in gravity (PJM 1871 – the coolest star, and PJM 1045 at 4400–4500 K, see Table 6), and the differences in gravity do not seem to be correlated with differences in abundances.

Carretta et al. (2005) provided a detailed comparison of their work with Friel et al. (2003). They showed that the equivalent widths of Friel et al. (2003) are systematically smaller for stronger lines (≳80 mÅ) for the lines in common (among which there are 24 Fe I lines). This could in part explain the lower metallicities. On the other hand, Carretta et al. (2005) used the Friel et al. (2003) equivalent widths and their own methods for the star with the largest abundance difference (PJM 2105), and derived an [Fe/H] value close to that obtained from their own data. They ascribed this to their different approach in estimating the microturbulent velocity (based on computed instead of observed equivalent widths). For the test star, the microturbulence derived by Carretta et al. (2005) is indeed 0.25 km s^{-1} lower. However, for two other stars with (smaller) abundance differences, the microturbulence is about 0.1 km s^{-1} higher.

De Silva et al. (2007) compared their results with those of Carretta et al. (2005), and noted that they are similar except for the coolest star with lowest gravity (PJM 1871). They also performed a test on three stars, using two different types of model atmospheres (Kurucz and MARCS, Asplund et al. 1997), and found that the differences in Fe abundance were lower than 0.03 dex.

Collinder 261 is a rather old OC, located in the inner disk, which makes it an interesting object for studying the evolution of metallicity distributions in the Galactic disk. It is included in the list of standard clusters proposed by Paunzen & Netopil (2006), with an age of 8.8 Gyr and a distance of 2.2 kpc. There is no photometric metallicity determination available, that is, it is not included in Paper I. Therefore, we used the method of Pöhnl & Paunzen (2010) (see also Sect. 4) to estimate its metallicity using B, V, I photometry, published by Gozzoli et al. (1996) and Phelps et al. (1994, V and I only). The Phelps et al. (1994) photometry was brought onto the scale by Gozzoli et al. (1996) by

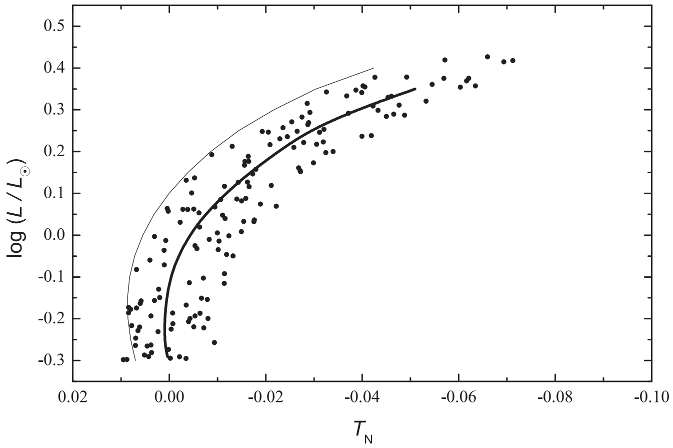

Fig. 8. Theoretical HR-diagram illustrating the photometric metallicity determination for Collinder 261 using the method by Pöhnl & Paunzen (2010). Logarithmic luminosity is plotted versus normalized logarithmic effective temperature, $T_{\rm N}$ = $\log T_{\rm eff} - \log T_{\rm eff}$(ZAMS), where $T_{\rm eff}$ (ZAMS) is the $T_{\rm eff}$ of a zero-age main-sequence with solar composition for a given luminosity (see Table 4 of Pöhnl & Paunzen 2010). Using the parameters by Paunzen & Netopil (2006), the metallicity was determined as Z = 0.021 ([Fe/H] ≈ 0.05 dex, isochrone shown as a thick line). In addition, the isochrone for Z = 0.012 ([Fe/H] ≈ −0.2, thin line) is shown, representing the high-resolution metallicity value of Friel et al. (2003).

applying corrections of +0.031 and +0.033 mag for V and $V-I$, respectively. An average and standard deviation of the photometry was calculated. We selected only stars available in both studies with errors <0.05 mag, covering the whole cluster. The colour–colour and colour-magnitude diagrams were examined to select most probable main-sequence cluster members.

The method is based on grids of evolutionary models, originally for [Fe/H] from −0.7 to +0.4 and ages up to 4 Gyr, which were extended to older ages using Geneva isochrones (Lejeune & Schaerer 2001). To transform $V-I$ into effective temperatures (in addition to $B-V$), the empirical relation for A to K dwarfs by Bessell et al. (1998) as well as their colour-excess ratios (including colour terms) were used.To transform the photometry into the $T_{\rm eff} - \log(L/L_{\odot})$ plane, the cluster parameters by Paunzen & Netopil (2006) were adopted. Since only $E(B-V)$ is tabulated, the temperatures deduced from $V-I$ were scaled to the $B-V$ results by applying an offset of −0.04 mag to the transformed reddening value. This offset can either be due to a small error in the calibration or to an abnormal reddening law in this direction. The final temperatures from both indices agree within <2%, and were averaged. All other steps of the method were applied as given in Pöhnl & Paunzen (2010).

In Fig. 8, the best-fit isochrone for the given parameters can be found, which results in a metallicity estimate of $Z = 0.021$ (heavy-element-mass fraction, corresponding to [Fe/H] ≈ 0.05 dex for $Z_{\odot}$ = 0.019 and a helium-mass fraction $Y = 0.23+2.25Z$). This supports the spectroscopic results around solar metallicity or higher. In addition, the low-resolution result by Friel et al. (2002) with [Fe/H] = −0.16 dex would support solar metallicity, when applying an ad-hoc correction of +0.2 dex, as suggested by comparison with high-resolution results (see e.g. Sect. 3.7).

In conclusion, we decided to disregard the determinations by Friel et al. (2003) for the computation of the average metallicity of Collinder 261 (Sect. 4) because of the lower resolution and the inconsistencies with the other three studies.

3.6. Other cases with high dispersion or large discrepancies

Melotte 20: the highest dispersion in the high-resolution sample occurs for Melotte 20 (α Per cluster), studied by Gonzalez & Lambert (1996, see Table 4) – 0.26 dex for three stars, one supergiant and two dwarfs. For one of the dwarf stars (HE 490), their result is close to the only other high-resolution study for four dwarf stars in this cluster (Boesgaard & Friel 1990), and to metallicity estimates from lower-resolution spectroscopy and photometry. The metallicity of the second dwarf star (HE 767) is about 0.2 dex higher. Gonzalez & Lambert (1996) discussed several possible explanations for this discrepancy, but did not find supporting evidence for any of them and concluded that the problem remains unresolved. The metallicity of the supergiant (α Per, $\log g$ = 1.2) is about 0.3 dex lower than that of HE 490. The authors ascribed this discrepancy to non-LTE effects, based on a contemporary estimation of these effects for metal-poor stars with similar $T_{\rm eff}$, but slightly larger $\log g$ (Lambert et al. 1996). We note that the Gonzalez & Lambert (1996) analysis used stellar-atmosphere models obtained from R. Kurucz in 1992, which assume plane-parallel geometry. However, the extended atmospheres of supergiants are more accurately described by spherical geometry. According to Heiter & Eriksson (2006), the inappropriate geometry leads to an overestimation of Fe abundances by ≈0.05 dex for the stellar parameters and Fe lines used by Gonzalez & Lambert (1996), that is, in the opposite direction of the non-LTE effect.

IC 4651: this cluster appears in four high-resolution studies (No. 16 in Table 4). In the study by Carretta et al. (2004), the large dispersion of 0.19 dex obtained for the average metallicity of five stars agrees with the individual errors quoted by the authors. However, the large dispersion is due to one star, a cool giant near the RGB tip (IC 4651 56, $\log g$ = 0.3). The metallicity of this star is about 0.4 dex lower than that of the other four stars, which are red clump stars. Again, the authors ascribed the discrepancy to non-LTE effects, supported by the large difference between spectroscopic and photometric (evolutionary) gravities determined for the RGB tip star. For this type of star, geometry only affects abundances derived from Fe II lines, which may be underestimated by ≈0.05 dex (Heiter & Eriksson 2006). The mean cluster metallicity quoted by the authors (0.11 ± 0.01 dex) is based on the four red clump stars. It has the smallest dispersion of the four studies and agrees perfectly with the others.

Collinder 121: only one star in this cluster, the supergiant HD 50877, has been studied by two authors. Mallik (1998) quoted [Fe/H] = +0.25, and Hekker & Meléndez (2007) obtained [Fe/H] = −0.32. They also quoted substantially different $T_{\rm eff}$ and $\log g$ values (3200 K/0.0 and 3900 K/0.65, respectively). As mentioned above, non-LTE effects are suspected to occur in the atmospheres of supergiants, and therefore these stars are poorly suited to estimate the metallicity of an OC.

NGC 2141: two different stars were studied in three publications (one each by Yong et al. 2005 and Jacobson et al. 2009, and both by Jacobson & Friel 2013). Both stars are bright giants ($\log g$ = 1.2). The first two works resulted in rather different metallicities (−0.18 ± 0.15 dex and +0.00 ± 0.16 dex, respectively). Although these values agree within the quoted errors, the large errors and the large discrepancy point to considerable uncertainties inherent in the atmospheric modelling of

Table 8. Abundance analyses of NGC 2632 stars (Praesepe) – mean [Fe/H] values and standard deviation, spectrum quality, approximate number of Fe I and Fe II lines used, and corresponding wavelength ranges.

				Fe I		Fe II	
[Fe/H]	Reference	R	S/N	n	λ [Å]	n	λ [Å]
Dwarfs							
+0.04 ± 0.03	Friel & Boesgaard (1992)	28k	100–200	7/14	7015–7205		
+0.11 ± 0.00	An et al. (2007)	55k	>100	15	5300–6200	9	4490–6150
+0.27 ± 0.04	Pace et al. (2008)	100k	≈80	60	4800–6800	10	4800–6800
Giants							
+0.15 ± 0.05	Carrera & Pancino (2011)	30k	150–215	177	5055–8945	9	5991–7711

these stars. Jacobson et al. (2009, Sect. 5.1.3) investigated this problem in more detail. They obtained the spectrum used by Yong et al. (2005) taken with the same instrument and setup, and two more spectra of the same stars with higher resolution, but lower S/N used by Bosler (2004), who had derived an even lower metallicity for the two stars. Analysing these spectra from scratch in the same way as their own observations, they arrived at a consistent metallicity close to solar. They demonstrated that different values for the microturbulence parameter are a major source for the abundance differences. Systematic differences in measured equivalent widths and different sets of spectral lines may contribute as well. Jacobson & Friel (2013) reanalysed the same spectra as were used in Yong et al. (2005) and Jacobson et al. (2009) with a new version of the radiative transfer code and more recent, spherical stellar atmosphere models than Jacobson et al. (2009). They obtained consistent metallicities of -0.09 ± 0.18 dex for the two stars, and for the Fe I and the Fe II line lists, that is, in between the previous discrepant determinations.

NGC 2632: for Praesepe, metallicity determinations are available for 15 different stars (three giants and twelve dwarfs) in four publications (No. 58 in Table 4). In each paper, a different set of stars was analysed, which makes a direct comparison impossible. The results in each of the three publications using dwarf stars show small dispersions for their respective stellar samples (at most 0.04 dex for two to six stars), but the mean metallicities are significantly different from each other (by 0.07 to 0.23 dex). The discrepancies might be due, apart from the different objects studied, to the different spectroscopic material, and the different selection of Fe lines used. In particular, the wavelength regions and spectral resolutions vary between the three works, while the S/Ns are similar (see Table 8). It is curious that the study based on the spectra with the highest resolution quotes the most discrepant value. The metallicity derived by An et al. (2007) for dwarf stars agrees best with the value obtained for giants by Carrera & Pancino (2011).

3.7. Importance of spectrum quality for mean cluster metallicity

We now turn from comparing determinations for individual stars to a comparison of mean cluster metallicities based on low-, medium- and high-resolution spectra, *all with high S/N*. We started from a list of 33 clusters studied at medium resolution ($13\,000 \leq R < 25\,000$) and searched for low- or high-resolution determinations for the same clusters. In total, we found multiple-resolution determinations for 23 clusters. Nineteen of these have determinations from low-resolution spectra (spectroscopic indices) in four publications. The medium-resolution determinations are taken from ten publications. The low- and medium-resolution references are listed in Table 9.

The cluster Tombaugh 2 is not included in Table 9. It is part of the Friel et al. (2002) sample, and has been studied at medium resolution by Frinchaboy et al. (2008) and Villanova et al. (2010). These two authors analysed 14 and 13 radial velocity members, respectively, using the same instrument, but different wavelength regions. Frinchaboy et al. (2008) obtained two different mean metallicities (about solar and −0.3 dex) for the two halves of their sample, while Villanova et al. (2010) arrived at a consistent metallicity of about −0.3 dex for all of their stars. The possible reasons for the different results are discussed at length in Villanova et al. (2010). We add that of the five stars in common between the two studies, one has the same atmospheric parameters and metallicity, while three have different parameters and metallicities, and one has different parameters but the same metallicity. We note in particular that the metallicity difference increases with the difference in microturbulence parameter between the two works. Two additional radial-velocity members of Tombaugh 2 have been analysed by Brown et al. (1996) at high resolution. However, no atmospheric parameters are given, and for the metallicity only the absolute value is quoted. Adopting the reference solar abundance for Fe I given in Brown & Wallerstein (1992), who used the same analysis methods, the metallicities of the two stars would be −0.6 and −0.8 dex. We regard the status of this cluster as inconclusive.

All but one cluster are included in the high-resolution sample (31 publications, see Table 4). Most of them have several different determinations that agree very well with each other. In Fig. 9, we plot the mean cluster metallicities from each publication as a function of reference [Fe/H] (between −0.25 and +0.15 dex), as given in Table 9. Two clusters at the two metallicity extremes lie outside of this range (NGC 2243 and NGC 6791).

The metallicities based on indices by Friel et al. (2002) are lower by up to 0.5 dex than the medium- and high-resolution metallicities (the differences increase with metallicity). This discrepancy has previously been noted for individual stars in representative clusters in Sects. 3.2 to 3.4, and by Pancino et al. (2010) for 28 OCs in the Friel et al. (2002) sample, which also have $R > 15\,000$ determinations (see also Friel et al. 2010, Sect. 6.1.3). A systematic difference of about 0.2 dex is also seen between the Friel et al. (2002) OC metallicities and metallicities compiled for Cepheids at similar Galactocentric distances (see Fig. 4 in Pedicelli et al. 2009). On the other hand, for NGC 6705 at [Fe/H] = 0.06 dex, both the Thogersen et al. (1993) and Marshall et al. (2005) indices result in higher metallicities than at high resolution, while for NGC 1245 (0.02 dex), NGC 2682 (0.03 dex), and NGC 6791 (0.42 dex), the determinations by Marshall et al. (2005) or Worthey & Jowett (2003) are about 0.1 dex lower than at high resolution.

The medium-resolution results agree in general very well with the high-resolution ones, except for IC 4756, NGC 188, NGC 2158, NGC 2420, and NGC 6705. For IC 4756

Table 9. Metallicities and references for medium- and low-resolution studies for clusters shown in Fig. 9.

Cluster ID	Ref. [Fe/H]	Mean [Fe/H]	std. dev.	Resolution	#	Star type	Reference
NGC 2243	−0.480	−0.42	0.05	18 000−20 000	10	giant	Jacobson et al. (2011a)
NGC 2243	−0.480	−0.49	0.05	1250	9	giant	Friel et al. (2002)
NGC 2204	−0.230	−0.23	0.04	20 000	13	giant	Jacobson et al. (2011a)
NGC 2204	−0.230	−0.32	0.10	1250	12	giant	Friel et al. (2002)
Berkeley 39	−0.220	−0.18	0.06	22 500	21	giant	Bragaglia et al. (2012)
Berkeley 39	−0.220	−0.26	0.09	1250	14	giant	Friel et al. (2002)
NGC 1817	−0.110	−0.16	0.03	18 000/21 000	28	giant	Jacobson et al. (2011b)
NGC 1817	−0.110	−0.29	0.05	1250	3	giant	Friel et al. (2002)
NGC 2194	−0.090	−0.08	0.08	18 000	6	giant	Jacobson et al. (2011b)
NGC 2158	−0.052	−0.25	0.09	1250	7	giant	Friel et al. (2002)
NGC 2158	−0.052	−0.28	0.05	14 500/21 000	15	giant	Jacobson et al. (2011b)
NGC 2355	−0.048	−0.08	0.08	18 000	5	giant	Jacobson et al. (2011b)
NGC 2420	−0.044	−0.20	0.06	18 000	9	giant	Jacobson et al. (2011b)
NGC 2420	−0.044	−0.38	0.07	1250	20	giant	Friel et al. (2002)
IC 2602	−0.020	−0.05	0.04	18 000	6	dwarf	Randich et al. (2001)
NGC 3532	+0.010	+0.07	0.06	18 000	5	giant	Luck (1994)
IC 4756	+0.018	−0.03	0.05	18 000	4	giant	Luck (1994)
IC 4756	+0.018	−0.15	0.04	15 000	6	giant	Jacobson et al. (2007)
IC 4756	+0.018	−0.25	0.08	1250	8	giant	Friel et al. (2002)
NGC 1245	+0.022	−0.04	0.05	18 000	13	giant	Jacobson et al. (2011b)
NGC 1245	+0.022	−0.14	0.09	1150	7	clump	Marshall et al. (2005)
NGC 6633	+0.026	−0.10	0.02	13 000	10	dwarf	Jeffries et al. (2002)
NGC 2682	+0.030	−0.01	0.05	14 500/18 000	19	giant	Jacobson et al. (2011b)
NGC 2682	+0.030	−0.05	0.04	1150	5	clump	Marshall et al. (2005)
NGC 2682	+0.030	−0.15	0.05	1250	25	giant	Friel et al. (2002)
NGC 7789	+0.040	+0.02	0.04	18 000	28	giant	Jacobson et al. (2011b)
NGC 7789	+0.040	−0.24	0.09	1250	57	giant	Friel et al. (2002)
NGC 6939	+0.050	−0.19	0.09	1250	4	giant	Friel et al. (2002)
NGC 6939	+0.050	+0.00	0.10	15 000	8	giant	Jacobson et al. (2007)
NGC 6705	+0.060	+0.14	0.16	1150	4	clump	Marshall et al. (2005)
NGC 6705	+0.060	+0.21	0.09	1200/2000	6	giant	Thogersen et al. (1993)
NGC 6705	+0.060	+0.23	0.13	24 000	6	giant	Gonzalez & Wallerstein (2000)
NGC 5822	+0.080	−0.21	0.10	1250	3	giant	Friel et al. (2002)
NGC 5822	+0.080	+0.09		18 000	1	giant	Luck (1994)
NGC 7142	+0.100	−0.10	0.10	1250	12	giant	Friel et al. (2002)
NGC 7142	+0.100	+0.08	0.06	15 000	6	giant	Jacobson et al. (2007)
NGC 188	+0.110	−0.03	0.04	18 000	27	giant	Jacobson et al. (2011b)
NGC 2112	+0.140	−0.36		1250	1	giant	Friel et al. (2002)
NGC 2112	+0.140	+0.02		16 000	1	giant	Brown et al. (1996)
NGC 6791	+0.420	+0.11	0.10	1250	39	giant	Friel et al. (2002)
NGC 6791	+0.420	+0.32	0.02	≈1000	14	giant	Worthey & Jowett (2003)
NGC 6791	+0.420	+0.42	0.05	15 000	16	giant	Geisler et al. (2012)

Notes. The second column lists the reference metallicity. The reference [Fe/H] values are the weighted means of high-resolution determinations for all stars in each cluster (cf. Table 1; IC 4756, NGC 1245, and NGC 6633, as well as NGC 2158, NGC 2355, and NGC 2420 were shifted for better visibility) or the medium-resolution determination for NGC 2204.

at 0.018 dex the work of Jacobson et al. (2007) gives a 0.15 dex lower metallicity value than the other medium-resolution publication and the three high-resolution publications. For NGC 188, NGC 2158, and NGC 2420 the medium-resolution values by Jacobson et al. (2011b) are 0.1 to 0.2 dex lower than the high-resolution determinations. For NGC 6705 at 0.06 dex, the medium-resolution value by Gonzalez & Wallerstein (2000) is 0.15 dex higher than two of the high-resolution values, while the high-resolution value of Santos et al. (2012) is lower than the other two by a similar amount, and all mean [Fe/H] values agree within the standard deviations.

NGC 2112 (reference [Fe/H] = 0.14 dex) has two discrepant high-resolution determinations. This old anticentre OC is useful for determining the radial metallicity gradient of the Galactic disk. Brown et al. (1996) found it to be mildly deficient, [Fe/H] = -0.16 ± 0.25 dex (only one star was observed at high resolution), while Carraro et al. (2008) found it to be slightly supersolar, [Fe/H] = +0.14 dex, close to the Hyades value. Brown et al. (1996) observed a cool red giant, while Carraro et al. (2008) observed one dwarf, one clump giant, and one F giant with a small dispersion of 0.03 dex.

NGC 6633 (reference [Fe/H] = 0.026 dex) has four discrepant high-resolution determinations. The closest [Fe/H] values, +0.03 dex for six measurements of three stars, and +0.11 dex for one star, are obtained by Santos et al. (2009) and Smiljanic et al. (2009), respectively. Valenti & Fischer (2005) observed the same star as Smiljanic et al. (2009), NGC 6633 100 = HD 170174, which is also in common with Santos et al. (2009), but derived the significantly higher value of +0.35 dex. The temperature adopted by Valenti & Fischer (2005) is substantially hotter ($T_{\rm eff}$ = 5245 K, while Smiljanic et al. 2009 adopted $T_{\rm eff}$ = 5015 K, and Santos et al. 2009 $T_{\rm eff}$ = 4980 K). We conclude that the different temperature scale employed by Valenti & Fischer (2005) is the cause for the

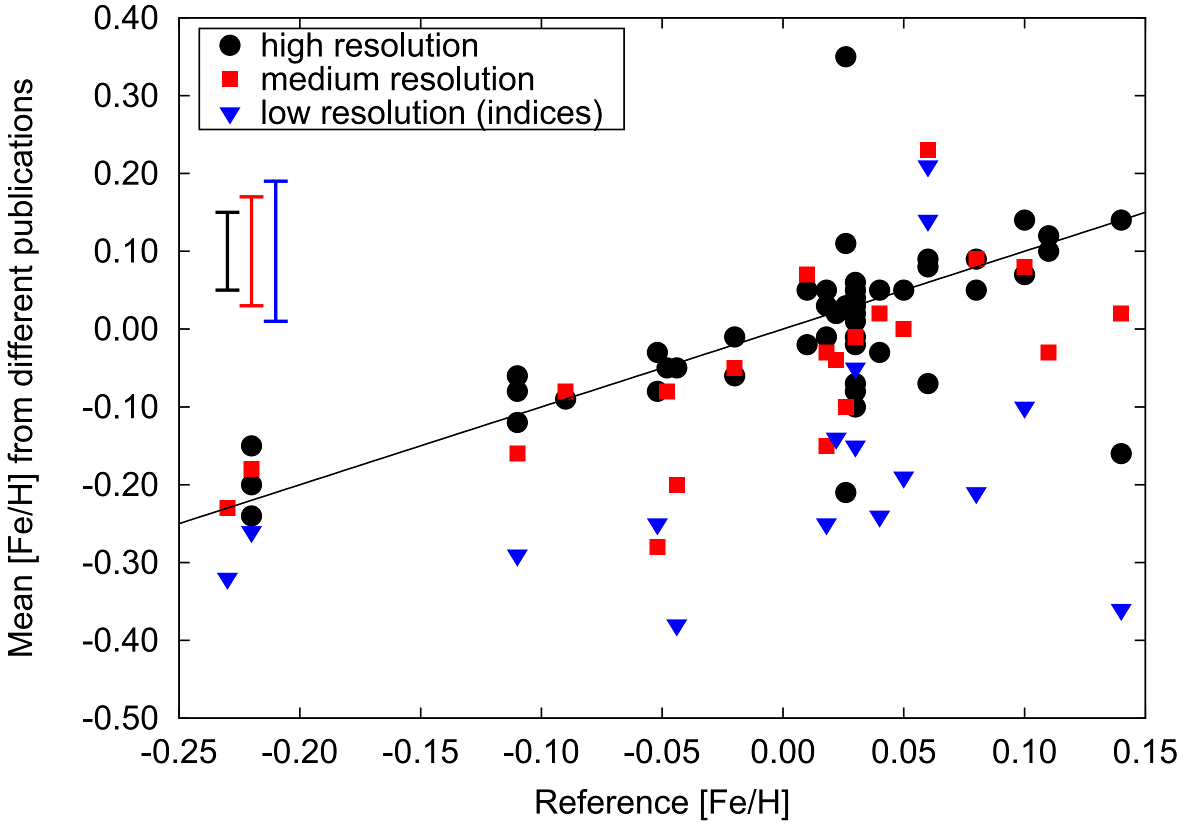

Fig. 9. Mean cluster metallicity determined by different authors from spectra with different resolution versus reference [Fe/H]. High resolution: $R \geq 25\,000$, medium resolution: $R \geq 13\,000$, low resolution: $R \approx 1000$, spectroscopic indices. All spectra have high S/N. The reference [Fe/H] values are given in Table 9. The solid line is the one-to-one relation. The bars below the legend represent the average standard deviations of the cluster means for high, medium, and low resolution from left to right, respectively. Metallicities and references for medium- and low-resolution studies are given in Table 9. Metallicities and references for high-resolution studies are given in Table 4.

discrepant metallicity determination. Therefore, we discarded this determination when we calculated the final mean cluster metallicity (Sect. 4). The fourth metallicity determination by Ashwell et al. (2005) is significantly lower than the others (−0.21 dex) and is based on two F dwarfs. The most metal-poor one (JEF 1), with [Fe/H] = −0.31 dex is a moderate rotator with $v \sin i$ = 19 km s^{-1} and a high $T_{\rm eff}$ = 6870 K, while the cooler F dwarf (HJT 1251 = JEF 16) has a value of [Fe/H] = −0.15 dex, which agrees better with the other determinations.

In summary, at resolutions higher than ∼10 000, cluster metallicities may have small or large dispersions regardless of the resolution value. Other factors such as analysis method, temperature scale, or properties of the sample stars seem to play a larger role for the reliability of the metallicity than spectral resolution.

Finally, we assessed the impact of S/N by comparing mean cluster metallicities determined by different authors from spectra with high (>50) or low S/N, *all of them with high resolution*. For six clusters we found metallicity determinations from both high-S/N spectra (21 publications) and low-S/N spectra (8 publications). The clusters, metallicities, and references for low-S/N determinations are given in Table 10. Metallicities and references for high-S/N determinations can be found in Table 4. For NGC 6475, the low-S/N determination results in a higher metallicity than the high-S/N determination, although the values agree within two standard deviations. For NGC 188, NGC 2243, and NGC 6791, the one or two low-S/N metallicities are lower than the one or two high-S/N ones for each cluster, but they agree within one standard deviation. For Berkeley 29 and NGC 2682, the one or two low-S/N determinations available for each cluster lie within the range of the high-S/N mean metallicities. Thus, spectra with a S/N as low as 20 might be sufficient to determine reliable cluster metallicities. However, the limited number of cases for comparison does not enable us to draw a firm conclusion.

4. Final high-resolution sample

To construct the final list of reference spectroscopic cluster metallicities, we retained the restrictions in spectral resolution and S/N, even thoug lower-quality spectra may also provide reliable results. For the high-quality sample we compiled the metallicity values for individual stars from the complete literature, while the lower-quality sample compiled by us is incomplete and comprises only average cluster metallicities.

Following the considerations in Sect. 3, we decided to restrict the temperature and gravity range of the determinations used to compute the average metallicity of each OC. We adopted the $T_{\rm eff}$ range 4400–6500 K with $\log g \geq 2.0$ to eliminate any rapidly rotating hot dwarfs or stars with chemical peculiarities, and bright giants possibly affected by non-LTE effects. When two or more determinations were available for the same star, with parameters on both sides of the limiting value, the star was included, but only determinations that met the constraints were included in the average metallicity (four dwarfs and ten giants in 12 clusters). For dwarfs, the lower $T_{\rm eff}$ limit eliminates three stars, without any critical consequence on the corresponding OCs (the metallicity of these cool dwarfs is very uncertain

Table 10. Metallicities and references for low-S/N studies for clusters discussed in Sect. 3.7, last paragraph.

Cluster ID	Mean [Fe/H]	std. dev.	Resolution	*S/N*	#	Star type	Reference
Berkeley 29	−0.32	0.03	45 000	25–50	5	giant	Sestito et al. (2008)
NGC 188	−0.12	0.16	≈30 000	≈45	7	dwarf+subgiant	Hobbs et al. (1990)
NGC 188	0.01	0.08	35 000–57 000	20–35	5	dwarf	Randich et al. (2003)
NGC 2243	−0.54	0.10	19 300/28 800[a]	30–40	76	dwarf+giant	François et al. (2013)
NGC 2682 (M67)	−0.04	0.01	≈30 000	30–45	2	dwarf	Hobbs & Thorburn (1991)
NGC 2682 (M67)	0.04	0.01	28 400	30–45	2	dwarf	Friel & Boesgaard (1992)
NGC 6475	0.11	0.03	40 000	20–30	10	dwarf	James & Jeffries (1997)
NGC 6791	0.30	0.08	45 000	40	2	turn-off	Boesgaard et al. (2009)

Notes. [(a)] Higher *R* between 638 and 663 nm, lower *R* between 660 and 696 nm.

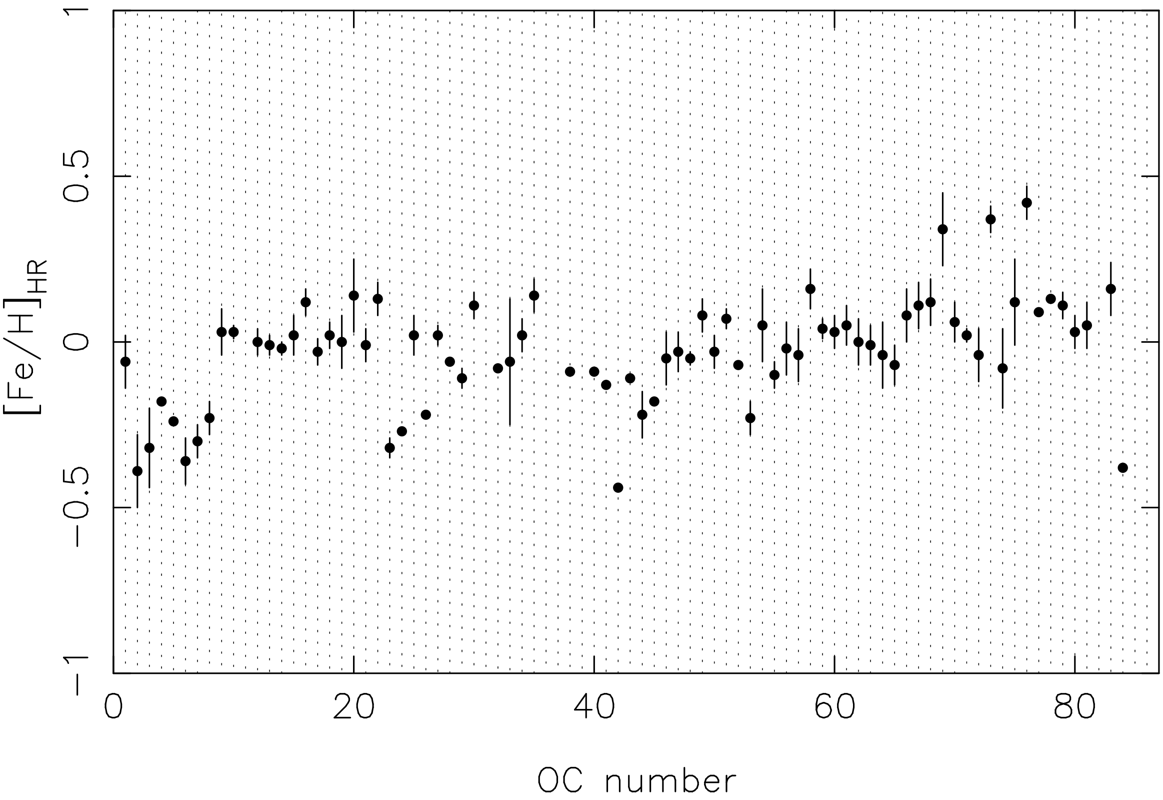

Fig. 10. Weighted average metallicity of OCs as listed in Table 11. The error bars represent the standard deviation of the mean.

anyway). The $T_{\rm eff}$ restriction is important to keep in mind for future metallicity calibrations, that is, the colour interval where they are valid. The $T_{\rm eff}$ restriction removed several clusters from the sample, namely Collinder 121 and NGC 2141 (see Sect. 3.6), as well as Pfleiderer 4, Trumpler 2, Trumpler 20, NGC 1883, NGC 2158, and the old OC NGC 2243. The latter is supposedly one of the most metal-deficient OCs according to the value of [Fe/H] = −0.48 dex determined by Gratton & Contarini (1994) for two bright giants.

Our final list includes 458 stars in 78 OCs, with 641 metallicity determinations corresponding to 86 papers. The measurements that are included in the final high-resolution sample are identified in Table 1. We computed the average metallicity from all determinations for each cluster, weighted by the inverse square of the individual errors quoted by the authors. For a significant number of determinations the authors did not quote any uncertainties. In these cases, we assumed an error of 0.1 dex.

This approach might seem problematic because authors did not compute the errors in the same way – some quoted only internal errors while others took some external sources of uncertainty into account. Therefore we tested several additional approaches to compute the average metallicity: a) setting the lower limit of the errors used for weighting to 0.1 dex (that is, the typical uncertainty due to the uncertainties in stellar parameters, see Sect. 3.1), and b) using equal weights for all metallicity values. The average metallicity values do not change by more than 0.03 dex for both approaches (a and b) for most clusters. They change by less than 0.1 dex for five and eight clusters (approaches a and b, respectively), with no systematic trend with metallicity. The standard deviations become larger (by more than 0.02 dex) for three clusters, and smaller for one cluster.

We tested another approach for computing the average cluster metallicity – a two-step mean, where we first calculated the mean metallicity for each star (we recall that a significant number of stars have been analysed by several authors), and then the mean for each cluster. Using this approach, only six clusters deviate from the nominal approach (by 0.02 dex), which shows that a straight one-step average is justified.

The resulting mean metallicities (one-step average with weights using the original errors) are plotted in Fig. 10 and

Table 11. Weighted average metallicity, and standard deviation, of OCs after restricting the $T_{\rm eff}$ and $\log g$ ranges, with the same running number for OCs as in Table 4. See also Fig. 10.

OC No.	Name	Mean [Fe/H]	#	n	OC No.	Name	Mean [Fe/H]	#	n
1	Berkeley 17	−0.06 ± 0.08	2	1	45	NGC 2335	−0.18	1	1
2	Berkeley 18	−0.39 ± 0.11	2	1	46	NGC 2355	−0.05 ± 0.08	3	3
3	Berkeley 20	−0.32 ± 0.12	2	2	47	NGC 2360	−0.03 ± 0.06	16	9
4	Berkeley 21	−0.18	1	1	48	NGC 2420	−0.05 ± 0.02	3	3
5	Berkeley 22	−0.24	1	1	49	NGC 2423	+0.08 ± 0.05	6	3
6	Berkeley 29	−0.36 ± 0.07	5	4	50	NGC 2447	−0.03 ± 0.05	18	3
7	Berkeley 32	−0.30 ± 0.06	15	11	51	NGC 2477	+0.07 ± 0.03	4	4
8	Berkeley 39	−0.23 ± 0.05	9	7	52	NGC 2482	−0.07	1	1
9	Blanco 1	+0.03 ± 0.07	6	6	53	NGC 2506	−0.23 ± 0.05	7	5
10	Collinder 110	+0.03 ± 0.02	3	3	54	NGC 2516	+0.05 ± 0.11	2	2
12	Collinder 261	+0.00 ± 0.04	14	13	55	NGC 2527	−0.10 ± 0.04	2	2
13	IC 2391	−0.01 ± 0.03	14	12	56	NGC 2539	−0.02 ± 0.08	8	4
14	IC 2602	−0.02 ± 0.02	10	7	57	NGC 2567	−0.04 ± 0.08	6	3
15	IC 2714	+0.02 ± 0.06	7	4	58	NGC 2632	+0.20 ± 0.09	14	14
16	IC 4651	+0.12 ± 0.04	35	18	59	NGC 2660	+0.04 ± 0.03	4	4
17	IC 4665	−0.03 ± 0.04	18	18	60	NGC 2682	+0.00 ± 0.06	52	27
18	IC 4756	+0.02 ± 0.04	22	15	61	NGC 3114	+0.05 ± 0.06	3	2
19	Melotte 111	+0.00 ± 0.08	13	10	62	NGC 3532	+0.00 ± 0.07	10	4
20	Melotte 20	+0.14 ± 0.11	2	2	63	NGC 3680	−0.01 ± 0.06	19	10
21	Melotte 22	−0.01 ± 0.05	12	10	64	NGC 3960	−0.04 ± 0.10	5	5
22	Melotte 25	+0.13 ± 0.06	92	61	65	NGC 4349	−0.07 ± 0.06	3	2
23	Melotte 66	−0.32 ± 0.03	6	6	66	NGC 5822	+0.08 ± 0.08	10	7
24	Melotte 71	−0.27	1	1	67	NGC 6134	+0.11 ± 0.07	8	8
25	NGC 1039	+0.02 ± 0.06	7	7	68	NGC 6192	+0.12 ± 0.07	3	3
26	NGC 1193	−0.22 ± 0.01	2	1	69	NGC 6253	+0.34 ± 0.11	12	10
27	NGC 1245	+0.02 ± 0.03	3	3	70	NGC 6281	+0.06 ± 0.06	2	2
28	NGC 1545	−0.06	1	1	71	NGC 6475	+0.02 ± 0.02	3	3
29	NGC 1817	−0.11 ± 0.03	7	4	72	NGC 6494	−0.04 ± 0.08	6	3
30	NGC 188	+0.11 ± 0.04	8	4	73	NGC 6583	+0.37 ± 0.04	2	2
32	NGC 1901	−0.08	1	1	74	NGC 6633	−0.08 ± 0.12	8	4
33	NGC 1977	−0.06 ± 0.19	2	2	75	NGC 6705	+0.12 ± 0.13	10	7
34	NGC 2099	+0.02 ± 0.05	3	3	76	NGC 6791	+0.42 ± 0.05	8	8
35	NGC 2112	+0.14 ± 0.05	3	3	77	NGC 6819	+0.09 ± 0.01	3	3
38	NGC 2194	−0.09 ± 0.00	2	2	78	NGC 6939	+0.13	1	1
40	NGC 2251	−0.09	1	1	79	NGC 7142	+0.11 ± 0.04	7	4
41	NGC 2264	−0.13	1	1	80	NGC 752	−0.02 ± 0.04	19	18
42	NGC 2266	−0.44	1	1	81	NGC 7789	+0.01 ± 0.04	6	5
43	NGC 2287	−0.11 ± 0.01	3	2	83	Ruprecht 147	+0.16 ± 0.08	5	5
44	NGC 2324	−0.22 ± 0.07	2	2	84	Saurer1	−0.38 ± 0.00	2	2

Notes. The column headed "#" gives the number of metallicity determinations, and the column headed "n" the number of individual member stars.

listed in Table 11. The figure can be directly compared with Fig. 1. For several clusters the standard deviations shown in Fig. 10 are smaller than the dispersion between different determinations for one and the same cluster seen in Fig. 1. This is most evident for No. 22 – Melotte 25 (the Hyades), and No. 74 – NGC 6633. For the Hyades, the largest number of metallicity determinations are available (129 in Table 4). After discarding 30% probably unreliable determinations, we are still left with a significant number (92 in Table 11), resulting in good statistics. The case of NGC 6633 is discussed in Sect. 3.7. Other clusters with improved dispersions are No. 6 – Berkeley 29, No. 12 – Collinder 261, No. 16 – IC 4651, No. 58 – NGC 2632, No. 60 – NGC 2682 (M67), No. 63 – NGC 3680, and No. 80 – NGC 752. In Fig. 11 we compare the average metallicities for the final sample with the weighted average metallicities per cluster for the starting sample, which includes all determinations for all highly probable members without restrictions on atmospheric parameters. The mean difference (final sample minus all members) is 0.01 ± 0.04 dex, with minimum and maximum differences of −0.10 and +0.18 dex, respectively. This shows that the metallicities do not change significantly by restricting the $T_{\rm eff}$ and $\log g$ ranges, except for a few clusters with large standard deviations. The cluster changing by the largest amount (+0.18 dex) is Melotte 20 (α Per cluster), discussed in Sect. 3.6.

At the metal-rich end of the metallicity distribution of the final sample, we find three OCs with extreme values: NGC 6253 ([Fe/H] ≈ +0.3 dex; Carretta et al. 2007; Sestito et al. 2007; Montalto et al. 2012), NGC 6583 ([Fe/H] ≈ +0.4 dex; Magrini et al. 2010), and NGC 6791 ([Fe/H] ≈ +0.4 dex; Gratton et al. 2006; Geisler et al. 2012). At the metal-poor end, there are eight OCs with metallicities of about −0.3 dex and below: Berkeley 18, Berkeley 20, Berkeley 29, Berkeley 32, Melotte 66, Melotte 71, NGC 2266, and Saurer 1. The metallicities of three of these clusters rely on a substantial number of stars: 11 stars in Berkeley 32, leading to [Fe/H] = −0.30±0.06 (Sestito et al. 2006; Carrera & Pancino 2011; Yong et al. 2012; Jacobson & Friel 2013), six stars in Melotte 66, leading to [Fe/H] = −0.32 ± 0.03 (Sestito et al. 2008), and four stars in Berkeley 29, leading to [Fe/H] = −0.36 ± 0.07 (Carraro et al. 2004; Sestito et al. 2008). On the contrary, the metallicity of Melotte 71 ([Fe/H] = −0.27) is based on only one very faint star, PJ 127, $V \simeq 17$, which has $T_{\rm eff}$ = 4610 K, $\log g$ = 2.16, and an uncertainty on the metallicity

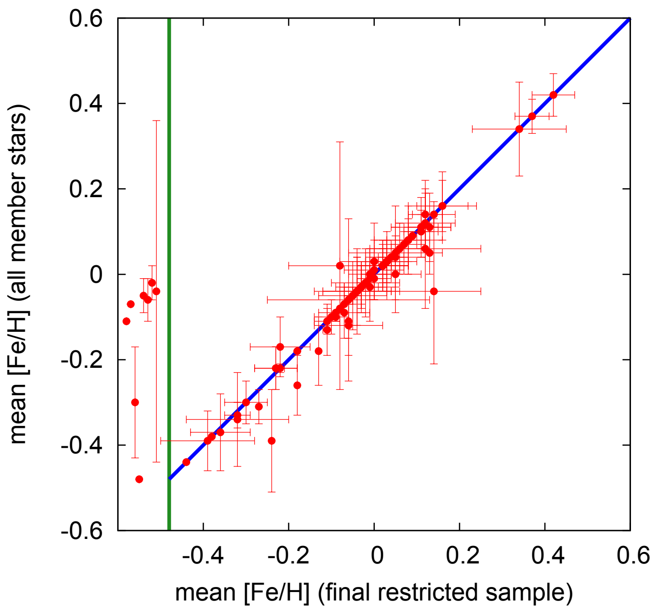

Fig. 11. Weighted average metallicity of OCs as listed in Table 11 versus weighted average metallicity of OCs, including all member stars from all publications in Table 4. The error bars represent the standard deviation of the mean. Clusters to the left of the green vertical line do not appear in the final sample.

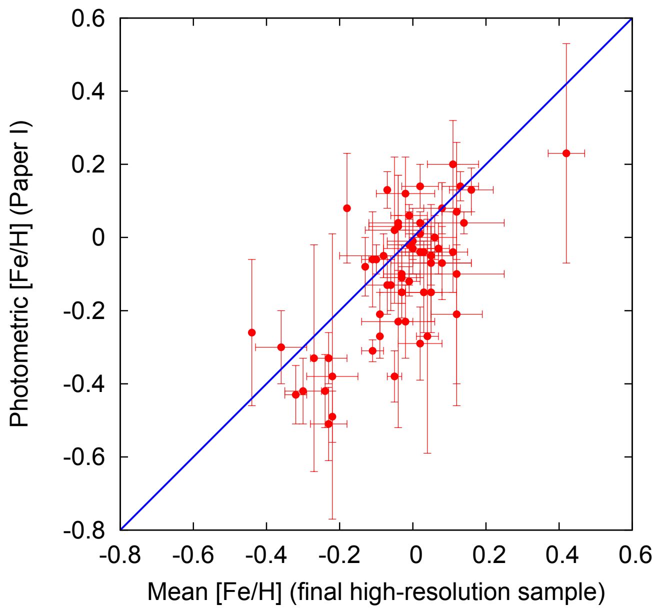

Fig. 12. Comparison of mean metallicities listed in Table 11 and those obtained from photometry in Paper I for 62 OCs in common (two clusters lie outside the axis ranges – No. 35, NGC 2112, and No. 4, Berkeley 21).

Table 12. Weighted mean metallicities and standard deviations for giant ($\log g \leq 3.0$) and dwarf samples in three clusters.

Name	Mean [Fe/H]	#
Melotte 25 giants	0.12 ± 0.04	16
Melotte 25 dwarfs	0.13 ± 0.06	76
NGC 2682 giants	−0.05 ± 0.05	23
NGC 2682 dwarfs	0.01 ± 0.06	29
IC 4651 giants	0.12 ± 0.05	15
IC 4651 dwarfs	0.12 ± 0.04	20

of 0.24 (Brown et al. 1996). NGC 2266 is the cluster with the lowest metallicity, [Fe/H] = −0.44, which is also based on only one star, although a brighter one ($V \simeq 11$) and with a lower uncertainty on the metallicity of 0.05 (Reddy et al. 2013). It is worth mentioning that the authors argued that this cluster may be part of the thick disk, based on its space motions. The low metallicity of Berkeley 18 is also based on one faint star, but two measurements (star K 1163 with $V \simeq 16$, see Sect. 3.4). The remaining two of the most metal-poor clusters (Berkeley 20 and Saurer 1) have metallicities relying on two stars. We have eleven more OCs in the final sample with metallicities relying on only one star, most of them with subsolar metallicities.

For the three clusters with the largest number of determinations (>30), we can separate the stars into giants ($\log g \leq 3.0$) and dwarfs (cf. Sect. 3.2 for M67). The weighted mean metallicities for the separated samples and the number of determinations are listed in Table 12. The determinations for the Hyades (Melotte 25) are mainly for dwarfs. For M67 (NGC 2682) and IC 4651, the determination numbers are more similar for giants and dwarfs. We found no indication for a metallicity difference between the dwarfs and giants for any of these clusters.

We compare in Fig. 12 the mean metallicities determined from high-resolution spectroscopy and that obtained from photometry (Paper I). There are 62 clusters in common, and the mean difference between photometric and spectroscopic values is −0.10 dex with a median of −0.08 and a standard deviation of 0.23. The two most extreme cases are NGC 2112 and Berkeley 21, with differences of −1.44 and −0.78 dex, respectively. These are also two of the most metal-poor clusters in the photometric sample ($[Fe/H]_{phot}$ = −1.30 and −0.96 dex, respectively). There are no other clusters with photometric metallicities below −0.5 dex in the common sample. We conclude that the photometric metallicity scale is more metal-poor than the spectroscopic one.

Combining our two samples of clusters with photometric and spectroscopic metallicities would result in a total number of 204 clusters with known metallicity. However, the differences in metallicity found for the two samples and the large intrinsic dispersion of the photometric determinations requires a calibration of the photometric sample to the spectroscopic metallicity scale. This process and the discussion of the full sample will be presented in a forthcoming article.

5. Discussion

5.1. Comparison with other metallicity studies

Netopil & Paunzen (2013) determined metallicities of 58 OCs from photometry, using an isochrone-fitting method developed by Pöhnl & Paunzen (2010). In Fig. 13 we compare the mean metallicities of the final high-resolution sample (Table 11) with the metallicities of Netopil & Paunzen (2013). We have 23 clusters in common with their sample, all of which have metallicities between −0.1 and +0.2 dex. The mean difference between the photometric and spectroscopic values is −0.02 ± 0.05 dex, with a maximum absolute difference of 0.09 dex. We confirm the conclusion of Netopil & Paunzen (2013) that their tool is useful for estimating OC metallicities from photometry.

A recent compilation of data, including metallicities, for a large number of OCs is the catalogue of Chen et al. (2003). A preliminary update is presented in Chen et al. (2009), which contains 144 clusters with metallicity, distance, and age values. However, the metallicities are a mixture of photometric and

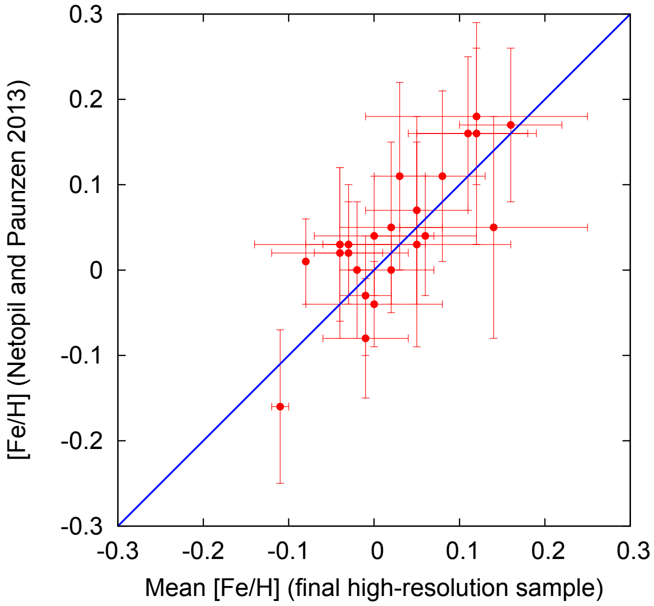

Fig. 13. Weighted average metallicity of OCs as listed in Table 11 versus metallicities determined by Netopil & Paunzen (2013).

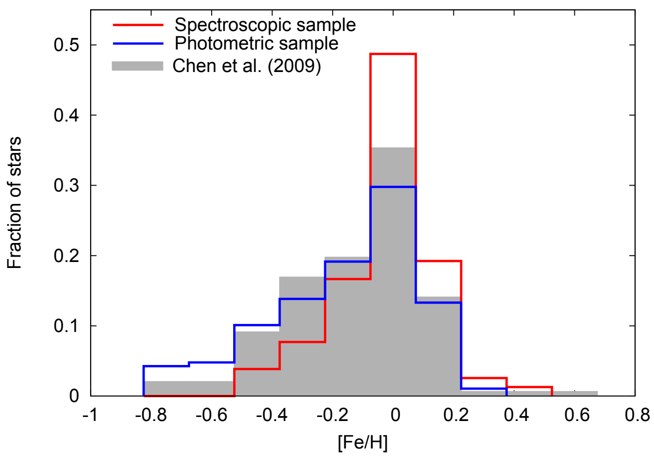

Fig. 14. Distribution of metallicities for the final spectroscopic sample (red line), the photometric sample (Paper I, blue line), and the sample of Chen et al. (2009, grey shaded histogram).

spectroscopic determinations. Figure 14 shows the histogram of cluster metallicities from Chen et al. (2009) together with those of our spectroscopic and photometric samples. The figure indicates that the peak at solar metallicity in the histogram of Chen et al. (2009) may be dominated by spectroscopic metallicities, while the metal-poor tail is mainly due to photometric metallicities.

In Fig. 15 we compare the mean metallicities of our final high-resolution sample with those compiled by Magrini et al. (2010, see Sect. 1). The mean difference for all clusters in common is 0.02 dex (median 0.00 dex), with a standard deviation of 0.05 dex. However, the dispersion varies with R_{GC}, and the lowest and highest values of the deviations are −0.10 and +0.16 dex, respectively. The scatter seen in this figure should be added to Fig. 9 of Magrini et al. (2010), representing the uncertainty originating from the way of combining cluster abundances from different authors. For example, the scatter is 0.06 dex for $7.5 \lesssim R_{GC} \lesssim 9.5$ kpc, adding to the uncertainty of the inner disk gradient determined by Magrini et al. (2010).

We have 64 clusters in common with the sample of Carrera & Pancino (2011, see Sect. 1). We do not show a detailed comparison of metallicities, since their sample is very similar to ours, and we included all of their references that meet our constraints. The differences are that their metallicities are based on published cluster means, not on individual stars, and that they set a lower limit on R (15 000) than we do, and no limit on S/N (spectra with S/N as low as 5 are included).

Ultimately, the OC metallicities should be combined with other tracers of metallicity in the Galaxy, such as HII regions, B-type stars, planetary nebulae, and Cepheids. However, such combined samples will have to deal with differences in metallicity scale, not only for the same type of objects due to different methods, but also between different types of objects. A large sample of Cepheids has been used by Pedicelli et al. (2009) to study the metallicity gradient of the Galactic disk. They compared the metallicities of their sample as a function of Galactocentric distance with several samples of OCs. They found significant differences in derived metallicity gradients, which were partly attributed to different Galactocentric distributions of these tracers.

It is worth noting that Pedicelli et al. (2009) combined spectroscopic metallicities for over 200 Cepheids with photometric ones for about 60. The mean difference between photometric and spectroscopic metallicities (−0.03 dex) and the intrinsic dispersion (0.15 dex) are smaller than for our two samples. This could partly be due to the more homogeneous photometric metallicities determined by Pedicelli et al. (2009) from one set of photometric bands (Walraven and K-band) and a metallicity calibration based on recent stellar evolution models. However, a systematic difference between two of their sources for spectroscopic metallicities is apparent in their Fig. 3.

5.2. Application to Galactic structure

In this section we use our final sample of OCs with spectroscopic metallicities for a preliminary investigation of the distribution of metals in the Galactic disk.

In Fig. 16 we show the spatial distribution of OCs projected onto the Galactic plane. Together with our final spectroscopic sample, we also include the photometric sample from Paper I and all clusters in the Dias et al. (2002, Version 3.2) catalogue. The metallicity of each cluster in the first two samples is indicated by the colour of the symbol. We recall that the photometric and spectroscopic metallicities are not yet on the same scale. Even though a combined sample would trace the metallicity throughout the disk better than the spectroscopic one alone, gaps are evident, which should be filled by targeted observations of known clusters. We did not attempt to derive a more detailed metallicity distribution for the spectroscopic sample in the immediate solar neighbourhood (±2 kpc), as we did in Fig. 4 of Paper I. The number of clusters in that area is simply too small (55 compared with 128 in Paper I). However, we speculate that the distribution based on a combined calibrated sample will be more smooth than that based on the photometric sample alone. In particular, the most distinct feature of Fig. 4 in Paper I, a dip in metallicity at $X = -8.4$ and $Y = -0.4$ kpc, will disappear. It is caused by the cluster NGC 2112, which has a spectroscopic metallicity of $+0.14 \pm 0.08$ dex, based on three stars in two publications, while its photometric metallicity of -1.3 ± 0.2 dex is based on Strömgren colours of four stars in one publication.

Figure 17 shows the cluster metallicity from Table 11 as a function of Galactocentric distance R_{GC} compared with the predictions of several models for Galactic chemical evolution.

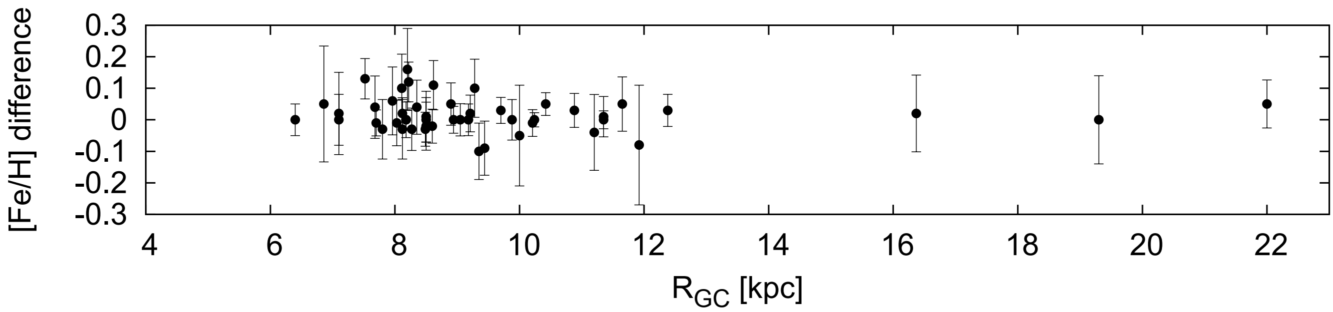

Fig. 15. Comparison of mean metallicities listed in Table 11 and those compiled by Magrini et al. (2010), for 49 OCs in common, as a function of Galactocentric distance. The points represent [Fe/H] (Magrini) minus [Fe/H] (this work). The error bars represent the standard deviations of the cluster means from both lists, added in quadrature. This can be directly compared with Fig. 9 of Magrini et al. (2010).

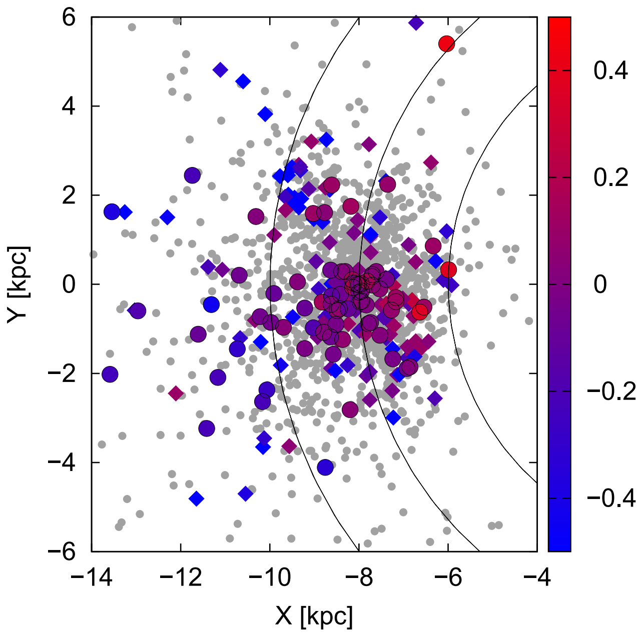

Fig. 16. Distributions of the OCs from Paper I (diamonds), the OCs in the spectroscopic sample (coloured circles), and the OCs in the Dias et al. (2002, version 3.2) catalogue (grey circles) projected onto the Galactic plane, in a linear coordinate system where X increases from the Sun towards the Galactic centre, and Y increases in the direction of Galactic rotation at the location of the Sun. The Galactic centre is located at $(X, Y) = (0,0)$. Metallicity is represented by the colour scale shown in the bar on the right. Solid lines indicate distances from the Galactic centre of 6, 8, and 10 kpc. Three clusters in the spectroscopic sample and one in the photometric sample lie outside the shown X range.

The Galactocentric distances were computed from the coordinates of the clusters and their distance from the Sun as given in the catalogue of Dias et al. (2002, version 3.2). The distance of the Sun from the Galactic centre is assumed to be $R_{\mathrm{GC},\odot} = 8$ kpc. The error bars for R_{GC} correspond to a variation of the cluster distances by ±20%. Most clusters are located in the range $6 \lesssim R_{\mathrm{GC},\odot} \lesssim 10$ kpc. The clusters within this range are also mostly located close to the Sun in the Galactic plane, as can be seen in Fig. 16, guided by the solid lines.

The metallicity distributions predicted by the following models are shown in Fig. 17:

- The *simple model* with instantaneous recycling described, for example, in Pagel (2009, Eq. (8.7)), long-dashed green line. This model allows one to derive an analytic expression for the average abundance of Fe in a stellar population:

$$\langle z(Fe)\rangle = 1 + \frac{\mu \ln(\mu)}{1-\mu},$$

where the gas fraction $\mu = g/(s+g)$, where g is the density of gas in the system, and s is the density of matter in the form of stars. The dependence of the gas fraction and, in turn, of the metallicity on R_{GC} is obtained by assuming the following relations for the gas and stellar surface densities in $M_\odot$ pc^{-2} as a function of Galactocentric distance in kpc:

$$g = 15.0\mathrm{e}^{\frac{-R_{\mathrm{GC}}}{9.9}}$$

(fit to data shown in Fig. 1 of Dame 1993, for $R_{\mathrm{GC}} > 4.5$ kpc), and

$$s = 198\mathrm{e}^{\frac{-R_{\mathrm{GC}}}{4.0}}.$$

The latter was normalized to give a gas fraction of 0.2 at the distance of the Sun (see Pagel 2009, Table 7.9).

- The *extreme inflow model*, with a metallicity dependence derived by Larson (1972) as:

$$\langle z(Fe)\rangle = 1 + \frac{1}{s/g(\mathrm{e}^{-s/g} - 1)}$$

(see Pagel 2009, Eq. (8.28)), short-dashed blue line.

- The model by Chiappini et al. (1997) – gradient of iron at 12 Gyr from their Table 4, but using $R_{\mathrm{GC},\odot} = 8$ kpc, dash-dotted grey line.
- The model by Naab & Ostriker (2006) – present-day metallicities of stars from their Fig. 11, solid red line.
- The model by Schönrich & Binney (2009) – mean metallicities of stars at the present time from their Fig. 11, solid black line.

Even though the first two analytical models can be regarded as two opposite extreme cases, their predicted radial dependence of metallicity is quite similar. It does not agree with the observed metallicity dependence, in particular at distances between about 10 and 15 kpc.

The main feature of the two-infall model by Chiappini et al. (1997) is that the thick and thin disks form by accretion of extragalactic material on very different timescales (1 Gyr and 8 Gyr, respectively). The model predictions agree well with several observed properties of the Galaxy, such as the stellar metallicity distribution and the fraction of metal-poor stars in the solar neighbourhood. However, the metallicity gradient predicted by the model is much shallower than that suggested by the OC metallicities (Fig. 17).

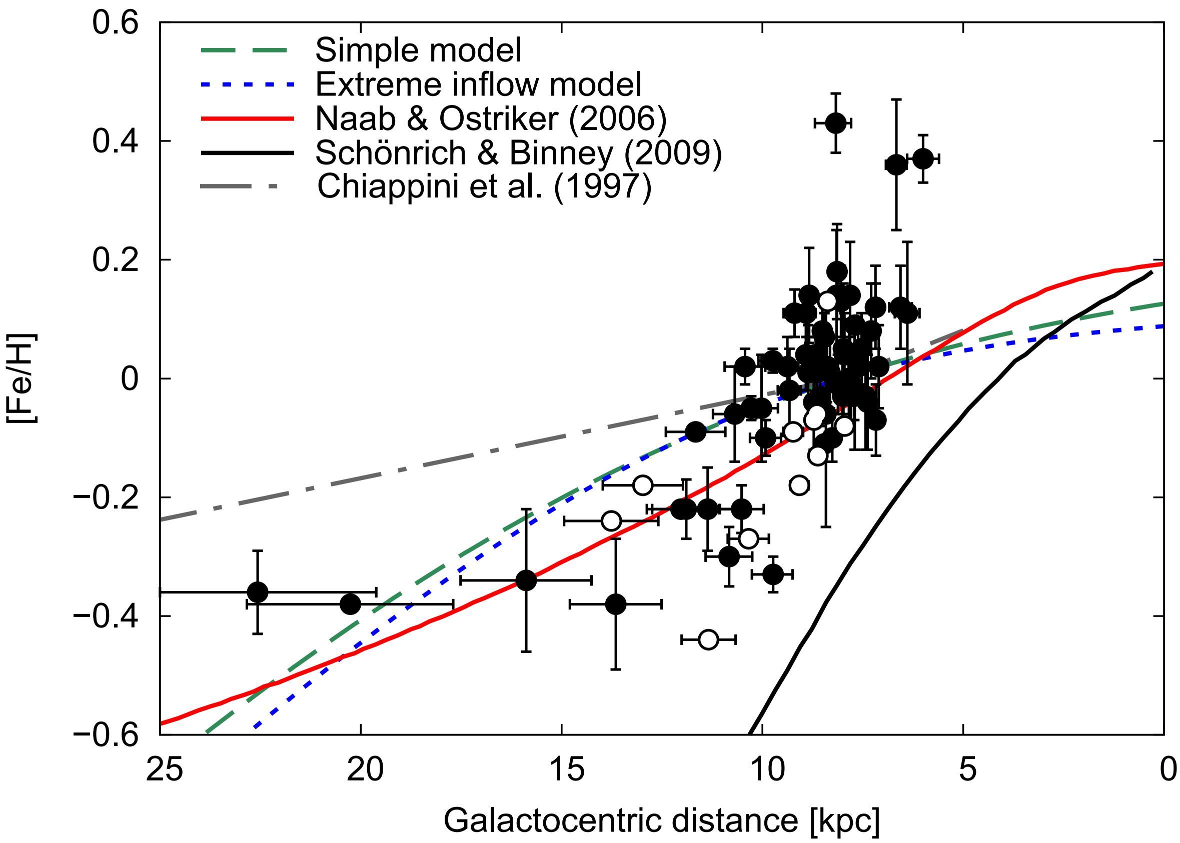

Fig. 17. Cluster metallicity as a function of Galactocentric distance computed from the coordinates of the clusters and their distance from the Sun taken from the Dias et al. (2002, version 3.2) catalogue. The distance of the Sun from the Galactic centre (at the right of the graph) is assumed to be 8 kpc. Open symbols are clusters with only one metallicity measurement. Also shown are predictions of several models for the Galactic chemical evolution. See Sect. 5.2 for details.

In the model of Naab & Ostriker (2006), the evolution of the gas infall rate is prescribed based on spherical infall theory and the current observed distribution of the total disk surface mass. For other ingredients (star formation, IMF, chemical evolution), the model uses standard prescriptions. Among the models discussed here, the radial dependence of metallicity predicted by this model agrees best with the OC metallicities, except that its metallicity is somewhat low at the solar radius. However, Naab & Ostriker (2006) mentioned that their model predicts a significantly steeper metallicity gradient for past times. Including information on the cluster ages might improve the agreement. Also, changing the IMF in the model from Salpeter (1955) to Chabrier (2003) leads to a steeper gradient.

The model of Schönrich & Binney (2009) introduces both radial gas flows and radial migration of stars, beyond the standard ingredients of chemical evolution models. This model predicts star counts as a function of various stellar parameters in agreement with observations, and it reproduces correlations between tangential velocity and abundance patterns. It also produces a thick disk alongside the thin disk within the Galaxy. Regarding the predicted metallicity as a function of $R_{\rm GC}$, the model curve does not coincide with any of the observed OC metallicities. To bring the model and observations into agreement would require a shift in metallicity of at least 0.3 dex. However, the model gradient is very similar to the observed one around the solar radius ($7 \lesssim R_{\rm GC} \lesssim 12$ kpc). The steep gradient is mainly caused by the radial gas flow, as Schönrich & Binney (2009) showed by varying the model parameters. Their model also predicts distributions over metallicity of stars at fixed $R_{\rm GC}$ with a full-width at half maximum (FWHM) around 0.35 dex. This value agrees exactly with the FWHM of the metallicity distribution of the 26 clusters in our sample with $7 \lesssim R_{\rm GC} \lesssim 9$ kpc.

Although the list of discussed models is not exhaustive, we can conclude that none of the current models for Galactic chemical evolution succeeds in predicting the metallicity gradient observed for the Galactic disk based on OCs. However, the significance of the comparison is limited by the inhomogeneous distribution of clusters over distance and the fact that the sample contains clusters of different ages. Moreover, we did not take into account possible radial migrations of the clusters. We postpone a more detailed comparison to a forthcoming paper, where we will combine the photometric and spectroscopic metallicity determinations in a proper way.

6. Summary and conclusions

For this article, metallicities of individual stars in OCs resulting from spectroscopy at high resolution ($R > 25\,000$) and high signal-to-noise ratio ($S/N > 50$) were exhaustively gathered from the recent literature (publication year 1990 and later). Only the most probable members in 86 OCs were considered for further analysis. Some discrepancies in metallicities of individual stars and cluster means were found for a fraction of OCs studied by several authors. The sources of these differences were analysed in relation to the quoted errors, and various aspects of the spectroscopic analyses with an impact on metallicity were discussed.

Comparisons were also made with metallicities based on lower resolution spectra and spectral indices, and on lower S/N observations. We found that low-resolution estimates are in general more metal poor than higher-resolution determinations. At medium and high resolution ($R \geq 13\,000$) and $S/N > 20$, the temperature scale, the line list, the methodology, and the choice of the microturbulence parameter, seem to play a larger role for the reliability of the metallicities than the resolution and S/N. However, the largest contribution to the observed dispersion comes from the properties of the stars. Chemically peculiar stars and binaries must obviously be removed when averaging the metallicity determinations in an OC, but also bright giants that are possibly affected by non-LTE, and hot dwarfs that are possibly affected by rapid rotation.

These considerations led us to build a clean sample of metallicity determinations of individual stars in a restricted temperature and gravity range, after rejecting some studies that appeared to be affected by systematic uncertainties. The numbers of different stars and metallicity determinations were reduced by 25% and nearly 30%, respectively, between the starting and the final sample. The final sample includes 458 stars with 641 metallicity determinations in 86 papers, which were used to compute the weighted average metallicity of 78 OCs. We found no difference in mean metallicities deduced from dwarfs and giants, based on three OCs with a significant number of determinations for both groups.

Photometric metallicities compiled in Paper I were found to be systematically more metal-poor by 0.11 dex than the spectroscopic ones presented here, with a standard deviation of 0.23 dex. However, recent photometric determinations by Netopil & Paunzen (2013) agree much better. The compilation of spectroscopic metallicities by Magrini et al. (2010), which consists of the cluster metallicity from one selected publication per cluster, agrees on average with our spectroscopic metallicities for the clusters in common. However, metallicities for individual clusters deviate by up to 0.16 dex.

We used our final sample to test four models that predict the radial metallicity gradient in the Galaxy. None of them was found to fully agree with the OC metallicities versus Galactocentric distance. The model by Schönrich & Binney (2009) has a similar slope, but shows a metallicity shift of 0.3 dex. The metallicity dispersion at the solar radius predicted by this model is similar to the one measured for our sample. This comparison shows that existing models of Galactic chemical evolution cannot reproduce the currently available sample of cluster metallicities even within the rather large observational uncertainties, and calls for further developments on the theoretical side.

This work demonstrates, however, that it is crucial to enlarge the number of OCs with accurate metallicities from spectroscopic studies. Metallicity determinations are needed in particular at small and large Galactocentric distances, and in several regions of the Galactic disk that are poorly sampled. To obtain reliable cluster metallicities will require an increase in the number of individual stars studied in each cluster, a careful selection of the stars, and a homogeneous analysis of the spectra. This is one of the main aims of the *Gaia*-ESO Public Spectroscopic Survey, which will dramatically improve the situation of spectroscopic metallicities of OCs, with 100 clusters to be observed in the next four years.

Studies of Galactic structure should take advantage of the large number of existing photometric metallicities for OCs (Paper I). In combination with the current spectroscopic sample, a sample of more than 200 clusters with known metallicities can be constructed. A calibration of the photometric sample using the spectroscopic sample will be required to define a common metallicity scale with a small intrinsic dispersion. The details of this calibration and the impact of the combined sample will be the subject of the next paper of this series.

Acknowledgements. U.H. acknowledges support from the Swedish National Space Board (Rymdstyrelsen). We thank the Bordeaux 1 University for providing U.H. a one-month position in 2009 and 2010. This work was supported by the SoMoPro II Programme (3SGA5916), co-financed by the European Union and the South Moravian Region, grant GA ČR 7AMB12AT003, and the financial contributions of the Austrian Agency for International Cooperation in Education and Research (CZ-10/2012). We thank the referee, Elena Pancino, for valuable comments. This research has made use of the WEBDA database, operated at the Department of Theoretical Physics and Astrophysics of the Masaryk University, and of the SIMBAD database, operated at the CDS, Strasbourg, France.

References

An, D., Terndrup, D. M., Pinsonneault, M. H., et al. 2007, ApJ, 655, 233
Ashwell, J. F., Jeffries, R. D., Smalley, B., et al. 2005, MNRAS, 363, L81
Asplund, M., Gustafsson, B., Kiselman, D., & Eriksson, K. 1997, A&A, 318, 521
Barrado y Navascués, D., Deliyannis, C. P., & Stauffer, J. R. 2001, ApJ, 549, 452
Bell, R. A., Eriksson, K., Gustafsson, B., & Nordlund, Å. 1976, A&AS, 23, 37
Bessell, M. S., Castelli, F., & Plez, B. 1998, A&A, 333, 231
Boesgaard, A. M., & Friel, E. D. 1990, ApJ, 351, 467
Boesgaard, A. M., Jensen, E. E. C., & Deliyannis, C. P. 2009, AJ, 137, 4949
Bosler, T. L. 2004, Ph.D. Thesis, University of California, Irvine, California, USA
Bragaglia, A., & Tosi, M. 2006, AJ, 131, 1544
Bragaglia, A., Carretta, E., Gratton, R. G., et al. 2001, AJ, 121, 327
Bragaglia, A., Tosi, M., Carretta, E., et al. 2006, MNRAS, 366, 1493
Bragaglia, A., Sestito, P., Villanova, S., et al. 2008, A&A, 480, 79
Bragaglia, A., Carretta, E., Gratton, R., & Tosi, M. 2009, in IAU Symp. 254, eds. J. Andersen, J. Bland-Hawthorn, & B. Nordström, 227
Bragaglia, A., Gratton, R. G., Carretta, E., et al. 2012, A&A, 548, A122
Brown, J. A., & Wallerstein, G. 1992, AJ, 104, 1818
Brown, J. A., Wallerstein, G., Geisler, D., & Oke, J. B. 1996, AJ, 112, 1551
Carraro, G., Bresolin, F., Villanova, S., et al. 2004, AJ, 128, 1676
Carraro, G., Villanova, S., Demarque, P., et al. 2006, ApJ, 643, 1151
Carraro, G., de La Fuente Marcos, R., Villanova, S., et al. 2007a, A&A, 466, 931
Carraro, G., Geisler, D., Villanova, S., Frinchaboy, P. M., & Majewski, S. R. 2007b, A&A, 476, 217
Carraro, G., Villanova, S., Demarque, P., Moni Bidin, C., & McSwain, M. V. 2008, MNRAS, 386, 1625
Carrera, R., & Pancino, E. 2011, A&A, 535, A30
Carretta, E., Bragaglia, A., Tosi, M., & Marconi, G. 2000, in Stellar Clusters and Associations: Convection, Rotation, and Dynamos, eds. R. Pallavicini, G. Micela, & S. Sciortino, ASP Conf. Ser., 198, 273
Carretta, E., Bragaglia, A., Gratton, R. G., & Tosi, M. 2004, A&A, 422, 951
Carretta, E., Bragaglia, A., Gratton, R. G., & Tosi, M. 2005, A&A, 441, 131
Carretta, E., Bragaglia, A., & Gratton, R. G. 2007, A&A, 473, 129
Castelli, F., Gratton, R. G., & Kurucz, R. L. 1997, A&A, 318, 841
Chabrier, G. 2003, PASP, 115, 763
Chen, L., Hou, J. L., & Wang, J. J. 2003, AJ, 125, 1397
Chen, L., Gao, X. H., & Zhao, J. L. 2009, in IAU Symp. 254, eds. J. Andersen, B. Nordström, & J. Bland-Hawthorn, 15
Chiappini, C., Matteucci, F., & Gratton, R. 1997, ApJ, 477, 765
Christian, C. A., & Janes, K. A. 1979, AJ, 84, 204
Cohen, J. G. 1980, ApJ, 241, 981
Cunha, K., Smith, V. V., & Lambert, D. L. 1995, ApJ, 452, 634
Curtis, J. L., Wolfgang, A., Wright, J. T., Brewer, J. M., & Johnson, J. A. 2013, AJ, 145, 134
D'Orazi, V., & Randich, S. 2009, A&A, 501, 553
da Silva, L., Girardi, L., Pasquini, L., et al. 2006, A&A, 458, 609
Dame, T. M. 1993, in Back to the Galaxy, AIP Conf. Ser. 278, eds. S. S. Holt, & F. Verter, 267
De Silva, G. M., Freeman, K. C., Asplund, M., et al. 2007, AJ, 133, 1161
De Silva, G. M., D'Orazi, V., Melo, C., et al. 2013, MNRAS, 431, 1005
Dias, W. S., Alessi, B. S., Moitinho, A., & Lépine, J. R. D. 2002, A&A, 389, 871
Edvardsson, B., Pettersson, B., Kharrazi, M., & Westerlund, B. 1995, A&A, 293, 75
Fagerholm, E. 1906, Ph.D. Thesis, Uppsala Univ., Sweden
Fernandez-Villacanas, J. L., Rego, M., & Cornide, M. 1990, AJ, 99, 1961
Ford, A., Jeffries, R. D., & Smalley, B. 2005, MNRAS, 364, 272
Foy, R., & Proust, D. 1981, A&A, 99, 221
François, P., Pasquini, L., Biazzo, K., Bonifacio, P., & Palsa, R. 2013, A&A, 552, A136

Friel, E. D. 1987, AJ, 93, 1388
Friel, E. D., & Boesgaard, A. M. 1992, ApJ, 387, 170
Friel, E. D., & Janes, K. A. 1993, A&A, 267, 75
Friel, E. D., Janes, K. A., Tavarez, M., et al. 2002, AJ, 124, 2693
Friel, E. D., Jacobson, H. R., Barrett, E., et al. 2003, AJ, 126, 2372
Friel, E. D., Jacobson, H. R., & Pilachowski, C. A. 2005, AJ, 129, 2725
Friel, E. D., Jacobson, H. R., & Pilachowski, C. A. 2010, AJ, 139, 1942
Frinchaboy, P. M., Marino, A. F., Villanova, S., et al. 2008, MNRAS, 391, 39
Gebran, M., & Monier, R. 2008, A&A, 483, 567
Gebran, M., Monier, R., & Richard, O. 2008, A&A, 479, 189
Gebran, M., Vick, M., Monier, R., & Fossati, L. 2010, A&A, 523, A71
Geisler, D., Villanova, S., Carraro, G., et al. 2012, ApJ, 756, L40
Gilmore, G., Randich, S., Asplund, M., et al. 2012, The Messenger, 147, 25
Gonzalez, G., & Lambert, D. L. 1996, AJ, 111, 424
Gonzalez, G., & Wallerstein, G. 2000, PASP, 112, 1081
Gozzoli, E., Tosi, M., Marconi, G., & Bragaglia, A. 1996, MNRAS, 283, 66
Gratton, R. G., & Contarini, G. 1994, A&A, 283, 911
Gratton, R., Bragaglia, A., Carretta, E., & Tosi, M. 2006, ApJ, 642, 462
Hamdani, S., North, P., Mowlavi, N., Raboud, D., & Mermilliod, J. 2000, A&A, 360, 509
Heiter, U., & Eriksson, K. 2006, A&A, 452, 1039
Hekker, S., & Meléndez, J. 2007, A&A, 475, 1003
Hill, V., & Pasquini, L. 1999, A&A, 348, L21
Hobbs, L. M., & Thorburn, J. A. 1991, AJ, 102, 1070
Hobbs, L. M., & Thorburn, J. A. 1992, AJ, 104, 669
Hobbs, L. M., Thorburn, J. A., & Rodriguez-Bell, T. 1990, AJ, 100, 710
Jacobson, H. R., & Friel, E. D. 2013, AJ, 145, 107
Jacobson, H. R., Friel, E. D., & Pilachowski, C. A. 2007, AJ, 134, 1216
Jacobson, H. R., Friel, E. D., & Pilachowski, C. A. 2008, AJ, 135, 2341
Jacobson, H. R., Friel, E. D., & Pilachowski, C. A. 2009, AJ, 137, 4753
Jacobson, H. R., Friel, E. D., & Pilachowski, C. A. 2011a, AJ, 141, 58
Jacobson, H. R., Pilachowski, C. A., & Friel, E. D. 2011b, AJ, 142, 59
James, D. J., & Jeffries, R. D. 1997, MNRAS, 292, 252
Jeffries, R. D., Totten, E. J., Harmer, S., & Deliyannis, C. P. 2002, MNRAS, 336, 1109
Jofre, P., Heiter, U., Soubiran, C., et al. 2013, A&A, submitted [arXiv:1309.1099]
King, J. R., & Hiltgen, D. D. 1996, AJ, 112, 2650
King, J. R., Soderblom, D. R., Fischer, D., & Jones, B. F. 2000, ApJ, 533, 944
Kurucz, R. 1993, ATLAS9 stellar atmosphere programs and 2 km s^{-1} CD-ROM No. 13 (Cambridge, MA: Smithsonian Astrophysical Observatory)
Lambert, D. L., Heath, J. E., Lemke, M., & Drake, J. 1996, ApJS, 103, 183
Larson, R. B. 1972, Nat. Phys. Sci., 236, 7
Lebzelter, T., Heiter, U., Abia, C., et al. 2012, A&A, 547, A108
Lejeune, T., & Schaerer, D. 2001, A&A, 366, 538
Luck, R. E. 1994, ApJS, 91, 309
Luck, R. E., & Challener, S. L. 1995, AJ, 110, 2968
Magrini, L., Sestito, P., Randich, S., & Galli, D. 2009, A&A, 494, 95
Magrini, L., Randich, S., Zoccali, M., et al. 2010, A&A, 523, A11
Mallik, S. V. 1998, A&A, 338, 623
Marshall, J. L., Burke, C. J., DePoy, D. L., Gould, A., & Kollmeier, J. A. 2005, AJ, 130, 1916
McWilliam, A. 1990, ApJS, 74, 1075
Meléndez, J., Asplund, M., Gustafsson, B., & Yong, D. 2009, ApJ, 704, L66
Mermilliod, J.-C., & Paunzen, E. 2003, A&A, 410, 511
Mermilliod, J. C., Mayor, M., & Udry, S. 2008, A&A, 485, 303
Mermilliod, J., Mayor, M., & Udry, S. 2009, A&A, 498, 949
Mikolaitis, Š., Tautvaišienė, G., Gratton, R., Bragaglia, A., & Carretta, E. 2011, MNRAS, 416, 1092
Mishenina, T. V., Soubiran, C., Kovtyukh, V. V., & Korotin, S. A. 2004, A&A, 418, 551
Mishenina, T. V., Bienaymé, O., Gorbaneva, T. I., et al. 2006, A&A, 456, 1109
Mitschang, A. W., De Silva, G. M., & Zucker, D. B. 2012, MNRAS, 422, 3527
Montalto, M., Santos, N. C., Villanova, S., et al. 2012, MNRAS, 423, 3039
Naab, T., & Ostriker, J. P. 2006, MNRAS, 366, 899
Netopil, M., & Paunzen, E. 2013, A&A, 557, A10
Pace, G., Pasquini, L., & François, P. 2008, A&A, 489, 403
Pagel, B. E. J. 2009, Nucleosynthesis and Chemical Evolution of Galaxies (Cambridge, UK: Cambridge University Press)
Pancino, E., Carrera, R., Rossetti, E., & Gallart, C. 2010, A&A, 511, A56
Pasquini, L., Randich, S., & Pallavicini, R. 2001, A&A, 374, 1017
Pasquini, L., Randich, S., Zoccali, M., et al. 2004, A&A, 424, 951
Paulson, D. B., Sneden, C., & Cochran, W. D. 2003, AJ, 125, 3185
Paunzen, E., & Netopil, M. 2006, MNRAS, 371, 1641
Paunzen, E., Heiter, U., Netopil, M., & Soubiran, C. 2010, A&A, 517, A32
Pedicelli, S., Bono, G., Lemasle, B., et al. 2009, A&A, 504, 81
Peterson, R. C., & Green, E. M. 1998, ApJ, 502, L39
Phelps, R. L., Janes, K. A., & Montgomery, K. A. 1994, AJ, 107, 1079
Platais, I., Melo, C., Mermilliod, J., et al. 2007, A&A, 461, 509
Platais, I., Melo, C., Fulbright, J. P., et al. 2008, MNRAS, 391, 1482
Pöhnl, H., & Paunzen, E. 2010, A&A, 514, A81
Ramírez, I., Allende Prieto, C., & Lambert, D. L. 2007, A&A, 465, 271
Randich, S., Pallavicini, R., Meola, G., Stauffer, J. R., & Balachandran, S. C. 2001, A&A, 372, 862
Randich, S., Sestito, P., & Pallavicini, R. 2003, A&A, 399, 133
Randich, S., Sestito, P., Primas, F., Pallavicini, R., & Pasquini, L. 2006, A&A, 450, 557
Reddy, A. B. S., Giridhar, S., & Lambert, D. L. 2012, MNRAS, 419, 1350
Reddy, A. B. S., Giridhar, S., & Lambert, D. L. 2013, MNRAS, 431, 3338
Salpeter, E. E. 1955, ApJ, 121, 161
Sanders, W. L. 1977, A&AS, 27, 89
Santos, N. C., Lovis, C., Pace, G., Melendez, J., & Naef, D. 2009, A&A, 493, 309
Santos, N. C., Lovis, C., Melendez, J., et al. 2012, A&A, 538, A151
Santrich, O. J. K., Pereira, C. B., & Drake, N. A. 2013, A&A, 554, A2
Schönrich, R., & Binney, J. 2009, MNRAS, 396, 203
Schuler, S. C., King, J. R., Fischer, D. A., Soderblom, D. R., & Jones, B. F. 2003, AJ, 125, 2085
Schuler, S. C., Hatzes, A. P., King, J. R., Kürster, M., & The, L. 2006, AJ, 131, 1057
Sestito, P., Randich, S., Mermilliod, J., & Pallavicini, R. 2003, A&A, 407, 289
Sestito, P., Randich, S., & Pallavicini, R. 2004, A&A, 426, 809
Sestito, P., Bragaglia, A., Randich, S., et al. 2006, A&A, 458, 121
Sestito, P., Randich, S., & Bragaglia, A. 2007, A&A, 465, 185
Sestito, P., Bragaglia, A., Randich, S., et al. 2008, A&A, 488, 943
Shen, Z., Jones, B., Lin, D. N. C., Liu, X., & Li, S. 2005, ApJ, 635, 608
Shetrone, M. D., & Sandquist, E. L. 2000, AJ, 120, 1913
Smiljanic, R., Gauderon, R., North, P., et al. 2009, A&A, 502, 267
Smith, G. 1999, A&A, 350, 859
Sneden, C. A. 1973, Ph.D. Thesis, Univ. Texas, USA
Sneden, C., Kraft, R. P., Prosser, C. F., & Langer, G. E. 1992, AJ, 104, 2121
Sobeck, J. S., Ivans, I. I., Simmerer, J. A., et al. 2006, AJ, 131, 2949
Soubiran, C., Odenkirchen, M., & Le Campion, J.-F. 2000, A&A, 357, 484
Soubiran, C., Le Campion, J., Cayrel de Strobel, G., & Caillo, A. 2010, A&A, 515, A111
Stetson, P. B., Bruntt, H., & Grundahl, F. 2003, PASP, 115, 413
Takeda, Y., Kawanomoto, S., Honda, S., Ando, H., & Sakurai, T. 2007, A&A, 468, 663
Tautvaišiene, G., Edvardsson, B., Tuominen, I., & Ilyin, I. 2000, A&A, 360, 499
Tautvaišienė, G., Edvardsson, B., Puzeras, E., & Ilyin, I. 2005, A&A, 431, 933
Terndrup, D. M., Pinsonneault, M., Jeffries, R. D., et al. 2002, ApJ, 576, 950
Thévenin, F., & Idiart, T. P. 1999, ApJ, 521, 753
Thogersen, E. N., Friel, E. D., & Fallon, B. V. 1993, PASP, 105, 1253
Thorén, P., & Feltzing, S. 2000, A&A, 363, 692
Ting, Y.-S., De Silva, G. M., Freeman, K. C., & Parker, S. J. 2012, MNRAS, 427, 882
Trundle, C., Dufton, P. L., Hunter, I., et al. 2007, A&A, 471, 625
Valenti, J. A., & Fischer, D. A. 2005, ApJS, 159, 141
Varenne, O., & Monier, R. 1999, A&A, 351, 247
Villanova, S., Carraro, G., Bresolin, F., & Patat, F. 2005, AJ, 130, 652
Villanova, S., Baume, G., & Carraro, G. 2007, MNRAS, 379, 1089
Villanova, S., Carraro, G., & Saviane, I. 2009, A&A, 504, 845
Villanova, S., Randich, S., Geisler, D., Carraro, G., & Costa, E. 2010, A&A, 509, A102
Worthey, G., & Jowett, K. J. 2003, PASP, 115, 96
Worthey, G., Faber, S. M., Gonzalez, J. J., & Burstein, D. 1994, ApJS, 94, 687
Wu, Z.-Y., Zhou, X., Ma, J., & Du, C.-H. 2009, MNRAS, 399, 2146
Yong, D., Carney, B. W., & Teixera de Almeida, M. L. 2005, AJ, 130, 597
Yong, D., Carney, B. W., & Friel, E. D. 2012, AJ, 144, 95
Začs, L., Alksnis, O., Barzdis, A., et al. 2011, MNRAS, 417, 649